Journal of Loss Prevention in the Process Industries 92 (2024) 105437

Contents lists available at ScienceDirect

Journal of Loss Prevention in the Process Industries

journal homepage: www.elsevier.com/locate/jlp

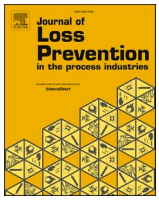

A risk assessment of a gas pressure reduction station system with confidence for dealing with imprecisions and unknowns

Batool Rafiee [a], Davood Shishebori [a], Edoardo Patelli [b,*]

[a] Department of Industrial Engineering, Yazd University, Yazd, Iran
[b] Department of Civil & Environmental Engineering, Strathclyde University, Glasgow, UK

ARTICLE INFO

Keywords:
Risk assessment
Uncertainty
Dempster-shafer theory
Credal network
FMECA
Belief and plausibility curves
City gate station

ABSTRACT

Process systems are sensitive and vital industrial facilities. Disturbances in their performance may cause harm to the environment,humans,or significant economic damage. In risk assessment of chemical process industries, the available data, information, and knowledge are typically rare, limited, and often unrealistic. This issue poses a challenge to conducting a credible quantitative risk assessment and effects the robustness of the results. To address these challenges, this work proposes a methodology based on the Dempster-Shafer theory of evidence as the reasoning framework. It incorporates risk identification, analysis, and mitigation phases to ensure a thorough analysis of risks and the integration of proactive risk reduction strategies. The approach aims to model the worst-case hazard scenario and assess associated risks using various methods such as FMECA, Bow-Tie, Credal Network, and Dempster-Shafer theory. The proposed approach models imprecision and data ambiguity using intervals and associated belief mass. This extension provides a basis for addressing the fundamental problem of prior ignorance about the distribution of the observed data, which is prevalent in data mining applications. A new approach is proposed that utilizes Belief and Plausibility curves, similar to a Cumulative Distribution Function, to propagate uncertainty, enhance criticality discrimination, and determine cumulated belief measures. This approach is applied in analyzing the failure modes identified in FMECA and is further extended through the credal network for comprehensive risk assessment. Results show how to express irrelevant and independent judgments, and how to work out with inferences in credal networks. This issue is often overlooked, but if properly addressed it represents the key to ultimately drawing reliable conclusions and fully utilizing the system's available data. A case study of the City Gate Station system was used to verify the application potential of the proposed approach.

1. Introduction

City Gate Stations (CGS) are crucial industrial facilities within the chemical process industries. This is due to their substantial storage of highly flammable and explosive materials. As potential sources of catastrophic accidents in urban areas, these stations have the capacity to significantly impact the general public (Karimi et al., 2022). Over the past few years, statistics have shown a significant increase in disastrous accidents from these stations (British Broadcasting Corporation, 2016). This incidents includes an explosion of a gas pipeline in Sarakhs' CGS station in 2010, fire and subsequent explosion in CGS of Tehran and Ghazvin province and Mobin petrochemical in 2016, a gas explosion in CGS of Hamedan province in 2017 in Iran. In such accidents, hundreds of people and crew members lost their lives and surrounding residential buildings sustained significant damage (British Broadcasting Corporation, 2016).

Once an accident falls out, the relevant department is quick to organize emergency meetings of domain experts to discuss and clarify treatment schemes. This is likely to be time-consuming and subsequently delay the best response time of hazard accident incidence, resulting in more severe losses (Schulman, 2023). To achieve a safe state of process systems, it is necessary to assess the risks of an accident before their occurrence and implement appropriate strategies for reducing the likelihood of hazards and mitigating potential undesired effects (Nguyen et al., 2022; Pasman et al., 2022; Ryu et al., 2023).

In process industries, hazardous events are fortunately infrequent due to the use of redundancies and sophisticated safety measures, which results in failure data at the system level being scarce. A particularly difficult problem for the area of safety engineering is to properly formulate quantitative analytic results without ignoring vital

* Corresponding author.
E-mail address: Edoardo.patelli@strath.ac.uk (E. Patelli).

https://doi.org/10.1016/j.jlp.2024.105437
Received 18 December 2023; Received in revised form 10 July 2024; Accepted 17 September 2024
Available online 22 September 2024

information and, on the other hand, without unjustified assumptions and simplifications. The industry standard techniques for risk assessment include the use of HAZard and Operational Process (HAZOP), Layers of Protection Analysis (LOPA), Failure Mode, Effect, and Criticality Analysis (FMECA), Bow-Tie analysis, fault tree analysis, event tree analysis, reliability graphs, reliability block diagram, GO-FLOW approach, and so on (Cameron and Raman, 2005; Yan and Xu, 2019). The usage of these techniques depends on the system as well as engineers' experiences. However, these conventional approaches have been widely criticized because of some drawbacks such as not enabling capturing the penurious knowledge and uncertainty that will lead to bias and inconsistent estimates of the risks (Ferson and Ginzburg, 1996). Consequently, if a robust strategy for characterizing uncertainty and lack of information is not achieved, risk or reliability results may expressively differ from reality, compromising any associated series of decisions relating to system safety with potentially serious consequences.

To address these challenges, there are robust methodologies available for uncertainty characterization and propagation, see e.g., (Aslett and Coolen, 2022; Faes et al., 2021; Gray et al., 2022). Among these methodologies, the Dempster–Shafer (D-S) evidence theory (Dempster, 2008; Sentz and Ferson, 2002; Shafer, 1976) has been proven to be an effective technique to handle subjective or non-specific (e.g., an expert's opinion) information, especially when there is not adequate data to specify events' probability distributions without further assumptions (Zhao et al., 2022). Theoretical justifications for its application exist (e.g., Dubois and Prade, 1986; Klawonn and Schwecke, 1992; Voorbraak, 1991). However, the D-S combination rule ignores conflicting evidence due to the presence of the normalization factor which associates the belief mass of conflict to the empty set. Following the work of (Sentz and Ferson, 2002), a procedure is proposed that does not require any aggregation stage and the input information is not forced to have non-empty intersections. Instead, all possible combination values among a specific parameter are considered to create the Belief and Plausibility curves forming the so-called probability boxes which represent the guaranteed bounds of the variable under consideration. Probability boxes offer a straightforward way to deal with inconsistent sources of information, overlapping and multiple intervals, as well as small sample sizes. The drawback of these approaches is that the computational cost of propagating these structures through the system is generally quite high, due to the necessity to compute the extreme of the response for each realization of these structures called focal elements. However, efficient non-intrusive sampling methods exist that are applicable to any model , e.g., (Patelli, 2015; Rocchetta et al., 2018).

Graphical models such as Credal Networks (CNs), i.e., a generalization of Bayesian Networks (Tolo et al., 2018a; Estrada-Lugo et al., 2020; Angelis et al., 2019) have gained increasing attention in safety analysis due to their flexibility to propagate different representations of uncertainty (Morais et al., 2019, 2021). Therefore, in this work, by leveraging the strengths of both approaches, tried to enhance the robustness and accuracy of risk assessments.

The proposed approach is utilized for the risk assessment of a CGS system. First, FMECA is used to determine the worst-case hazard scenarios based on previous work by some of the authors (Rafiee et al., 2019, 2020). Then, a Bow-Tie model (Cockshott, 2005) is employed for cause-consequence analysis of the hazard scenario and mapped into its equivalent CN (Hugo et al., 2022; Mauá and Cozman, 2020). Mapping Bow-Tie into CN allows accounting for dependencies among variables and the possibility of dealing with imprecision or partial availability of data. For further verification of the study, a sensitivity analysis (SA) is conducted. The approach allows the suggestion of mitigation strategies that can lessen the frequencies of the hazard scenario occurrence and its resulting consequences.

This paper is organized as follows: In section 2, an overview of the proposed framework is presented while details of the D-S theory are included in Appendix A.1. Section 3 shows the risk assessment of a City Gate Station, demonstrating the applicability of the approach to study real case examples. Section 4 summarizes the main findings and presents the advantages and limitations of the approach. Section 5 presents the conclusion of the paper. To demonstrate the usefulness of the proposed methodology in real industrial contexts affected by the presence of uncertainty, it is applied to the CGS system of the gas industry.

2. Proposed methodology

2.1. Overview

The proposed approach as shown in Fig. 1 consists of three main phases: 1) risk identification, 2) risk analysis, and 3) risk mitigation (i.e., analysis and proposition of preventive measures). All the above-mentioned risk phases involve an aggregation phase.

2.2. Aggregation phase

Mathematical details and definitions of D-S theory are reported in Appendix A.1 while for the sake of clarity, a brief explanation and a simple example are reported here.

Let's assume that three experts are provided the analysis of the probability of an event E, $P(E)$. $P(E)$ may be the probability of failure of a component and its values are shown in Table 1. In addition, each expert hastheir own confidence and expertise level. The confidence in the analysis is represented by the size of the interval provided, i.e., the distance between the belief interval, $[Bel(P(E)), Pl(P(E))]$, while the expertise level is mapped into a weighting factor (in Dempster rule of aggregation it is the basic probability assignments).

In risk analysis, the focus is often on identifying failures and examining worst-case scenarios. Therefore, the quantity of interest is believed to be the largest value of $P(E)$. This allows the aggregation of the information via the concept of cumulative distribution function generalized to Dempster-Shafer structures where the focal elements (belief intervals) are placed on the x-axis and the cumulative basic probability assignments on the y-axis using Eqs (A.5-A.6) (Yager, 1986).

The contribution of each belief interval is weighted according to the reliability of the sources as:

$$m_{1,\dots,n}(E) = \frac{1}{n}\sum_{i=1}^{n} w_i m_i(E) \tag{1}$$

where m_i is are the basic probabilistic assignment, BPA, for the belief structures being aggregated and the w_i's are the weight of each expert. By summing the masses of all those intervals m_i that are completely contained (Eq. (2)) or intersect (Eq. (3)) the interval $[0,E^*]$, the *Belief* and *Plausibility* curves are computed, respectively:

$$Bel(E) = Bel(\mathrm{E} \le \mathrm{E}^*) = \sum\nolimits_{m_{i\subset[0,\mathrm{E}^*]}} m_i(\mathrm{E}) \tag{2}$$

$$Pl(E) = Pl(\mathrm{E} \le \mathrm{E}^*) = \sum\nolimits_{m_{i\cap[0,\mathrm{E}^*]}} m_i(\mathrm{E}) \tag{3}$$

The aggregation of belief intervals delivered in Table 1 is provided in Table 2.

In often convenient to work with the complementary of the event E, i.e., $\overline{E} = \{E > E^*\}$. *Belief* and *Plausibility* become:

$$Bel(\overline{E}) = Bel(\mathrm{E} > \mathrm{E}^*) = 1 - Pl(\mathrm{E} \le \mathrm{E}^*) \tag{4}$$

$$Pl(\overline{E}) = Pl(\mathrm{E} > \mathrm{E}^*) = 1 - Bel(\mathrm{E} \le \mathrm{E}^*) \tag{5}$$

The resulting belief and plausibility curves shown in Fig. 2.

2.3. Risk identification

Risk identification is performed based on the FMECA approach to

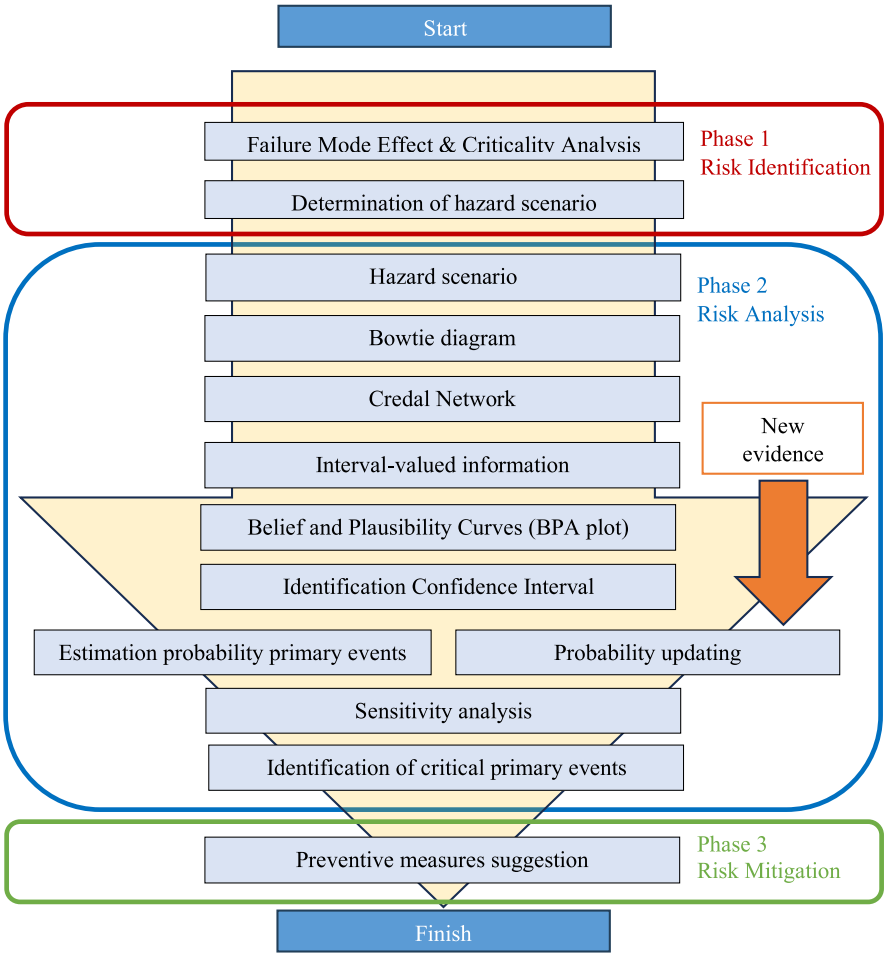

Fig. 1. Proposed methodology framework.

Table 1
Experts' judgment for a generic event E.

Experts	Interval	Weight
A	[0.01, 0.02]	50%
B	[0.015,0.02]	25%
C	[0.025, 0.03]	25%

Table 2
Aggregation of belief intervals.

$P(E) < P(E)^*$	Plausibility	Belief
0	0	0
0.01	0.5	0
0.015	0.75	0
0.02	0.75	0.75
0.025	1	0.75
0.03	1	1

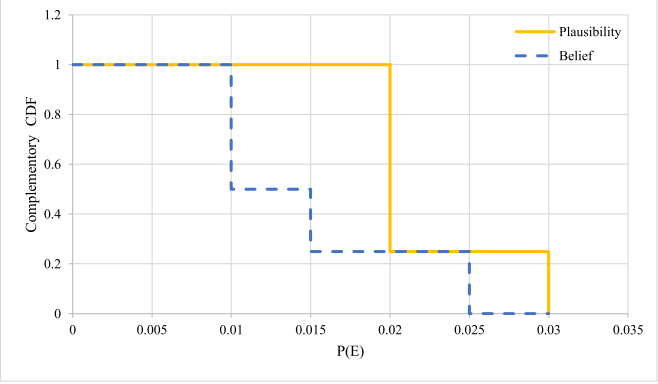

Fig. 2. Belief and Plausibility curves for the belief interval.

recognize failure modes (usually identified by experts). It also provides a qualitative analysis by the specification of occurrence (O), severity (S), and detection (D) based on a ten-point scale aligned with International Standard IEC 60812 (International Electrotechnical Commission, 2006). From their product, the risk priority number (RPN) is formed allowing for ranking the severity of different failure modes (a higher RPN indicates a more severe failure mode). When the values of O, S, and D are associated with intervals, the RPNs are calculated by the combining the products of the individual parameters. Therefore, $RPN_{i,r}$ is used to represent the RPN values for the i-th failure mode of the r-th combination and $m(RPN_{i,r})$ its corresponding mass calculated according to Eq. (1).

After computing all combined RPN values, the Belief and Plausibility functions for each failure mode are calculated based on Eqs. (2) and (3), resulting in a probability box (similar to the plot in Fig. 2). Then, the prioritization of failure modes is performed.

The strategy adopted is as follows. The failure mode with the highest potential value of RPN at a given level of confidence or consensus is the one desired to be identified using the aggregation strategy (Section 2.2). Hence, a credibility level $Pl(\overline{E}_i) = Y$ is used to identify the corresponding upper bound, i.e., $\overline{RPN_i^*}$ is obtained (if the $Bel(\overline{E}_i)$ =Y is used, the lower

bound $\underline{RPN_i^*}$ can be obtained).

The failure mode with the greatest $\overline{RPN^*}$ represents the worst-case hazard scenario and it is selected for a comprehensive and detailed risk analysis of the next phases of the study. Therefore, failure modes are sorted in descending order. The value of $Bel(\overline{RPN_i^*})$ is then used as the second criterion in the prioritization (again in descending order). The second criteria means that if two failure modes have the same value of $\overline{RPN^*}$, the failure mode with a larger Belief value is prioritized.

2.4. Risk analysis

The development of a Bow-Tie model was undertaken to illustrate the accident scenario identified in the previous phase. This model showcases the logical relationship between primary events, safety barriers, and potential consequences through the use of AND and OR gates. Safety barriers are physical and/or non-physical measures implemented to prevent, mitigate, or control undesired accidents or events (Hosseinnia Davatgar et al., 2021). The construction of the Bow-Tie model involves mapping out the primary events leading to the identified hazard scenario on the left side of the diagram. These events are connected by logical gates to safety barriers positioned in the central part of the diagram. Safety barriers represent preventive or mitigative measures, including actions by prevention systems, operators, safety warning systems, emergency control systems, manual operations, automated risk reduction facilities, and personnel responsible for safety protocols.

The right side of the Bow-Tie model shows the potential consequences resulting from breaches in the safety barriers. These consequences are linked by OR gates to the primary events and safety barriers, illustrating the pathways through which an accident scenario could manifest. By visually representing the interplay between primary events, safety barriers, and consequences, the Bow-Tie model provides a comprehensive overview of the risk landscape and enabling stakeholders to assess the effectiveness of existing safety measures and identify areas for improvement.

The Bow-Tie model is then mapped into its equivalent Credal Network (CN) using the mapping algorithm proposed by (Misuri et al., 2018). The mapping is based on two steps approach: a graphical representation and a numerical computation (Bobbio et al., 2001). In the graphical representation, the primary events of Bow-Tie make the primary nodes of CN while the top events of logical gates become the child nodes of the primary nodes in the CN. Safety barriers and consequences are also converted into their corresponding CN nodes.

For numerical computation, the probabilities of primary events in a Bow-Tie are assigned to probabilities of primary nodes in a CN. The logical gates defined by the Bow-Tie model produce conditional dependencies among intermediate events and these dependencies are captured by the CPTs at the corresponding child nodes of the CN. In this work, the Noisy-OR (Noisy-AND) model is used to represent the logical OR (AND) gate and to capture the non-determinism in a system (Bobbio et al., 2001). This is obtained by replacing the conditional probability of success to be 1 with probability λ_i, and failure 0 with probability $(1-\lambda_i)$ as shown in Table 3.

The prior probabilities along with amended CPTs are incorporated into the CN model as evidence for credal inference, allowing the calculation of the likelihood of an accident and its consequences. In order to determine the prior probabilities of primary events, Belief and Plausibility distributions are constructed based on the available information, facilitating a comprehensive synthesis of data. An arbitrary confidence level (e.g., 90%) of Plausibility distribution is used to identify the upper bound of the probability of the primary event as threshold i.e., $\overline{PE_i^*}$ (the lower bound can be calculated using the Belief function).

Table 3
Mapping of "AND" and "OR" gate in CPTs of Credal Network using noisy model.

A		Success		Failure	
B		Success	Failure	Success	Failure
TOP (AND)	**Success**	λ_i	$1-\lambda_i$	$1-\lambda_i$	$1-\lambda_i$
	Failure	$1-\lambda_i$	λ_i	λ_i	λ_i
TOP (OR)	**Success**	λ_i	λ_i	λ_i	$1-\lambda_i$
	Failure	$1-\lambda_i$	$1-\lambda_i$	$1-\lambda_i$	λ_i

These values are then used in the commercial software GeNie to evaluate the corresponding Bayesian Network (i.e., CN are reduced to Bayesian Network when intervals reduce to crisp values). Credal Networks enable imprecision in the probability of events, dependencies among events, and modeling cascading events to be considered. This allows to design and identify preventive measures. In fact, once an accident takes place, it is necessary to determine the most contributing cause events (Li et al., 2020a, 2020b). The diagnosis analysis conducted in the study is based on backward reasoning where the posterior probability of each risk factor (or sequence of events) was obtained and thereby the associated risk factors that contribute to the incidence of a hazard scenario.

Finally, sensitivity analysis (SA) is used to provide insights into model robustness. By evaluating the impact of changes in the input parameters on a model output of interest, one can verify that the model responds as expected and is valuable for model validation. For instance, in a robust model, the output would be sensitive, but would not show abrupt variationwith any individual minor changes in the input (Razavi et al., 2021; Saltelli et al., 2008). Efficient computational methods for SA are available, see e.g., (Patelli et al., 2010) and sensitivity assessment of CN involving probability bounds that have been performed by (Morais et al., 2022; Tolo et al., 2018b). Hence, as the last step of the study, SA is performed to validate the study's accuracy to confirm the previously identified variables that strongly affected the system's behavior in the occurrence of an accident.

The sensitivity parameter D(SA) is computed as:

$$D(SA) = \frac{\Delta P_t}{\Delta PE_i} \tag{6}$$

where Δ Pt and ΔPE_i are the changes in the target node's probability and in the i-th primary events, respectively.

2.5. Risk mitigation

This phase focuses on suggesting effective measures to avoid, reduce, eliminate, compensate, or control the negative consequences of hazard scenarios. The implementation of effective mitigation strategies contributes to preventing any hazard occurrence from breaking out in the first place. However, only a few published articles have currently addressed suggesting mitigation measures for CGS hazards (Heydari et al., 2022; Nourian et al., 2019). For this purpose, team members and specialists attended specific meetings to discuss the risk results obtained from previous phases. The meetings provided opportunities for sharing personalized and specific information from domain experts to suggest some necessary actions to lessen the frequency of discovered contributing factors and subsequently the occurrence of the worst-case hazard scenario and its resulting consequences.

3. Methodology application

3.1. Case study: a city gate station

Natural gas is produced from onshore and offshore natural oil and gas wells and coalbeds and afterward in the refinery is converted to sweet gas which can be used by consumers. Since the refinery is far from the end-user consumption, the natural gas transfers via transmission pipelines (Arya et al., 2023). The long-distance between refineries and consumption points like cities and industrial plants poses significant

challenges to the required pressure needed to overcome the losses along the path. Therefore, the pressure of natural gas at the transmission pipeline inlet is much higher than the required pressure at consumption points, and there are several booster and attenuator pressure stations along this way (Arabkoohsar et al., 2016). Along the transmission system near the consumption points, CGS is located to regulate the gas pressure to be used by consumers.

A typical CGS is composed of several physical arrays of filters, pipes, valves, and pressure reduction devices (regulators) devised to meter and reduce the gas pressure so as to safely deliver to customers through distribution networks. The natural gas is first purified using several filters to remove contaminants and impurities and reduce the potential negative impacts on the station's equipment. During the process of pressure reduction (i.e., gas expansion), the gas temperature drops. To prevent the formation of hydrates and negative icing effects, multiple heaters are used. Then, the gas is conducted to the transmission pipelines, each having dedicated regulators to reduce the gas pressure to a lower level (Arya et al., 2023). At the next level, the gas is conducted to the Town Boundary Stations. A typical CGS configuration and its main parts are shown in Fig. 3.

3.2. Expert details

An experienced multi-disciplined team composed of three safety and process experts in the field was established. As shown in Table 4, professional position, years of experience, level of education, and age are the four factors considered in the calculation of experts' weight (Ramzali et al., 2015). Although it is desirable to have access to a large number of experts, in practice their number is always very limited to between 3 and 15 with an optimal number of 6 according to (Budescu and Chen, 2015) but also affected by practicalities (e.g., cost expert availability). Based on weighting scores delivered in Table 5, the involved experts' corresponding weighting scores were calculated as 0.33 for each as they were assessed as equally reliable and credible.

3.3. Phase1: risk identification

3.3.1. FMECA

This step was performed in a previous study by some authors of this paper (Rafiee et al., 2019, 2020) and summarized here for completeness. Meetings and brainstorming sessions were held by experts and 23 potential failure modes were identified along with their associated causes and effects. Then, the identified failure modes were addressed and synthesized via FMECA as described by (Rafiee et al., 2019, 2020). Table 6 shows the identified failure modes. Table 7 synthesizes the judgments of experts on risk factors related to each failure mode

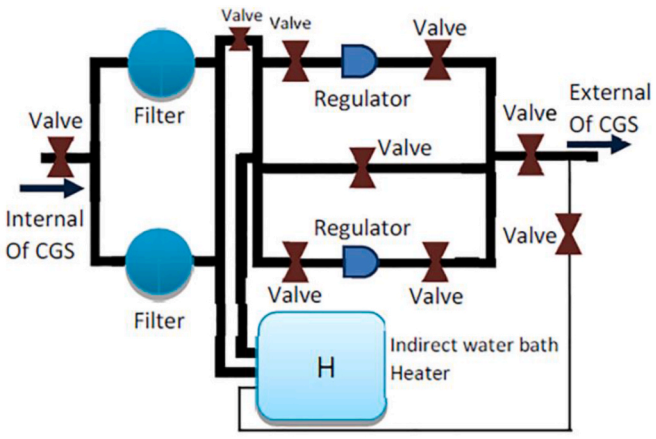

Fig. 3. A simplified configuration of a typical CGS (reproduced with permission from Mostafavi and Shirazi, 2020).

Table 4
Experts' weighting scores (Ramzali et al., 2015).

Index	Classification	Score	Index	Classification	Score
Professional position	Senior academic	5	Years of experience	30 ≥	5
	Junior academic	4		20–29	4
	Engineer	3		10–19	3
	Technician	2		6–9	2
	Worker	1		≤ 5	1
Level of education	PhD	5	Age	>60	5
	Master	4		50–59	4
	Bachelor	3		40–49	3
	Higher National Diploma	2		30–39	2
	School level	1		<30	1

bounded in the interval [1,10]. The three involved experts were considered equally reliable and credible (see section 3.2). Therefore, a mass of 1/3 was subjectively assigned to each expert estimation of specific risk factors. There were three experts with three risk factors for each failure mode, corresponding to $3^3 = 27$ combinations for every failure mode. For the sake of space limitation, only the analysis of failure mode 15 is reported and the 27 combinations generated are shown in Table 8. Subsequently, the Belief and Plausibility distribution functions were developed utilizing the data provided in Table 8 and following Eqs. (2) and (3). These functions are visually represented in Fig. 4.

A confidence level of 90%, i.e., the value of the plausibility function equal to 0.9, was used to define the threshold value of the failure mode 15, i.e., $\overline{RPN^*_{15}}$, corresponding to a value 126.

Failure mode prioritizing: The value of RPN_i corresponding to 90% confidence was calculated for each failure mode. The upper bound, indicated as $\overline{RPN^*_i}$, was obtained from the *Plausibility* function (the lower bound $\underline{RPN^*_i}$ could be obtained from the *Belief* function although not directly used here). The failure modes were ranked firstly according to $\overline{RPN^*_i}$ and, as a second criterion, from the value of the belief function corresponding to the upper bound $\overline{RPN^*_i}$. For instance, $Bel(\overline{RPN^*_4}) = 0$ while $Bel(\overline{RPN^*_3}) = 0.148148$, therefore it can be concluded that FM_4 is more critical than FM_3. The result can be seen in Fig. 5. The same procedure was applied for all failure modes and the ranking is reported in Table 9.

As shown in Table 9, FM_{21} (i.e., *Gas emission through replacement operation of filter's element)* was identified as the most critical, with an upper bound of the Risk Priority Number estimated at 400 with 90% confidence (i.e., $\overline{RPN^*_{21}} = 400$) and a Belief value of 0.222222. In contrast, FM_{20} (i.e., *Leakage of filter's gas throughout repairment*) although with $\overline{RPN^*_{20}} = 400$, has a *Belief* value of 0. Therefore, there is less belief that FM_{20} is as severe as FM_{21}. It is important to note that FM_{21} was not previously analyzed in previous studies (Rafiee et al., 2019, 2020).

3.4. Phase 2: risk analysis

3.4.1. Bow-Tie construction

After consulting experts and reviewing safety standards, the potential risk factors involved in the worst-case hazard scenario were identified and the causal relationships between them were established. Subsequently, the risk model of the hazard scenario was built up based on Bow-Tie methodology to explicitly depict the failure mode FM_{21} "*Gas emission through replacement operation of filter's element*", as the hazard scenario.

The Bow-Tie model contains 41 primary events, 16 intermediate events, 4 safety barriers, and 7 consequences as shown in Fig. 6. The causes of hazard scenario were categorized into two main groups:

Table 5
Experts' information and corresponding weighting scores.

Expert No	Title	Professional position	Level of education	Years of experience	Age	Weighting factor	Weighting score
1	Maintenance manager	Senior academic	Bachelor	21	48	15	0.33
2	Process inspector	Senior academic	Bachelor	22	49	15	0.33
3	Process site safety engineer	Junior academic	PhD	11	45	15	0.33

Table 6
Identified failure modes in CGS system (Rafiee et al., 2020).

Failure mode	Descriptions
FM_1	Heater coil's perforation
FM_2	Thermocouple rod's failure or ionization
FM_3	Heater's malfunction
FM_4	Gas leakage from heater's exterior part
FM_5	Electrical valves' malfunction
FM_6	Compressor's malfunction
FM_7	Electrical motor's malfunction
FM_8	Emission of odorant in surroundings
FM_9	Odorizer's panel malfunction
FM_{10}	Electricity existence in the body of the odorizer's panel
FM_{11}	Electricity existence in the body of the odorizer's control panel
FM_{12}	Odorizer's injection system malfunction
FM_{13}	Leakage of odorant through ventilation of odorizer
FM_{14}	Odorant's barrels perforation
FM_{15}	Abrasion, pipe wall weakening, pipe thickness, and perforation
FM_{16}	Fitting and pipeline's gas leakage
FM_{17}	Pipes and fittings vibration
FM_{18}	Rupture of sensing
FM_{19}	Detachment of sensor tubes
FM_{20}	Leakage of filter's gas throughout repairment
FM_{21}	Gas emission through replacement operation of filter's element
FM_{22}	Combination of gas with oxygen sited in the separator's bottom
FM_{23}	Filter separator's tech not fastening

human operational errors and mechanical failure. These main groups were further broken down into primary and intermediate events leading to hazard scenario occurrence. The descriptions of primary events and safety barriers are represented in Table 10.

In response to the occurrence of FM_{21}, where flammable substances accumulate in the CGS area, safety barriers are put in place to prevent or reduce the potential consequences of this failure mode, such as fire hazards. These safety measures effectively address the issue of flammable substance accumulation and ensure a safer environment.

As shown in the right part of the Bow-Tie model (Fig. 6), there are four categories of barriers, including Emergency Shutdown Barrier (ESB), Immediate Ignition Barrier (IIB), Delayed Ignition Barrier (DIB), and Congestion existence Barrier (CongB). Each category of safety barriers serves a specific purpose, but those barriers work together sequentially and in coordination to address risks and ensure a comprehensive response. For instance, in the event of a sudden increase in gas leakage, the ESB would automatically trigger the shutdown procedure, isolate affected areas, close gas valves, and activate alarms to alert personnel. By swiftly halting operations and containing the gas leak, the ESB is intended to prevent further escalation of the incident and set the stage for subsequent safety measures. If a spark or ignition source is detected near a CGS despite the activation of the ESB, the IIB would respond by sounding alarms, detecting the source, and activating fire suppression systems. This rapid elimination of the ignition risk would complement the actions of the ESB and prevent fires or explosions from occurring.

Following the successful mitigation of the ignition hazard by the IIB, the DIB comes into play in the event of a pipeline leak that releases flammable gas. Its intent is to introduce a time delay between leak detection and potential ignition to allow operators to assess and address the leak. This allows operators to isolate the leak, conduct repairs, and prevent the formation of an explosive gas mixture. Finally, the Congestion existence barrier facilitates the orderly evacuation of personnel by managing congestion, maintaining clear evacuation routes, and directing personnel away from the hazardous zone in case of a fire in a processing area while managing the gas leak with the DIB.

Overall, by working sequentially and complementing each safety barrier's functions, a robust safety system was created that integrates preventive, reactive, and responsive measures to effectively manage and mitigate the impact of incidents.

For each safety barrier, two outcomes were considered leading to

Table 7
Experts' judgments about failure modes' risk factors (Rafiee et al., 2020).

FM_i	Detection			Occurrence			Severity		
	Expert1	Expert2	Expert3	Expert1	Expert2	Expert3	Expert1	Expert2	Expert3
FM_1	[3,5]	5	[3,5]	[4,6]	6	[6,7]	[4,6]	[6,7]	[4,6]
FM_2	[3,5]	5	5	[5,6]	6	[4,7]	[6,8]	[7,8]	7
FM_3	[2,4]	5	[4,5]	[4,6]	[5,6]	5	[4,5]	[4,5]	5
FM_4	[2,4]	[4,5]	[4,6]	[4,5]	[5,6]	[4,5]	[2,5]	[4,5]	5
FM_5	[6,8]	8	[6,7]	[4,5]	7	[4,6]	[8,9]	9	[8,9]
FM_6	[1,3]	[1,3]	[3,4]	[2,4]	4	[4,5]	[6,7]	[6,7]	8
FM_7	[1,3]	[1,3]	[3,4]	[2,4]	3	[3,4]	[6,7]	[6,8]	[6,7]
FM_8	[3,4]	[4,6]	[3,4]	[4,5]	[4,5]	[5,6]	[3,4]	4	[4,5]
FM_9	[2,3]	4	[3,4]	[2,4]	[2,4]	4	[6,7]	[6,7]	6
FM_{10}	[3,4]	4	[4,5]	[3,4]	4	[4,5]	[8,10]	[9,10]	9
FM_{11}	[1,3]	3	[3,4]	[2,4]	4	[3,4]	[8,10]	[8,9]	[8,9]
FM_{12}	[1,3]	[2,3]	4	[5,7]	[5,6]	5	[6,7]	7	[5,7]
FM_{13}	[1,3]	[3,4]	[1,3]	[6,7]	7	[5,7]	4	4	[4,5]
FM_{14}	[1,3]	[2,4]	[4,5]	[6,7]	6	[6,7]	[4,6]	6	6
FM_{15}	**[3,5]**	**[3,4]**	**3**	**[4,6]**	**[5,6]**	**7**	**[5,7]**	**7**	**7**
FM_{16}	[2,4]	[2,4]	2	[3,4]	4	[4,5]	[2,5]	4	[4,5]
FM_{17}	[2,4]	4	[3,4]	[5,7]	8	[7,8]	8	[8,10]	[8,10]
FM_{18}	[1,3]	[2,3]	3	7	7	[7,8]	[7,9]	9	[7,8]
FM_{19}	[3,4]	4	[2,3]	5	5	[5,7]	[7,9]	[8,9]	[8,9]
FM_{20}	[4,5]	7	[5,6]	[8,9]	[7,9]	8	[8,10]	[8,10]	[8,10]
FM_{21}	[4,5]	5	[5,6]	[8,9]	[7,9]	8	[8,10]	[8,10]	9
FM_{22}	[2,4]	4	[4,5]	8	[8,10]	8	[8,10]	9	[7,8]
FM_{23}	[2,4]	[2,4]	5	[8,9]	8	7	9	9	[8,9]

Table 8
Expert's judgment's combination for failure mode 15.

Combination Number	Detectability	Occurrence	Severity	Risk Priority Number
1	[3,5]	[4,6]	[5,7]	[60,210]
2	[3,5]	[4,6]	[7,7]	[84,210]
3	[3,5]	[4,6]	[7,7]	[84,210]
4	[3,5]	[5,6]	[5,7]	[75,210]
5	[3,5]	[5,6]	[7,7]	[105,210]
6	[3,5]	[5,6]	[7,7]	[105,210]
7	[3,5]	[7,7]	[5,7]	[105,245]
8	[3,5]	[7,7]	[7,7]	[147,245]
9	[3,5]	[7,7]	[7,7]	[147,245]
10	[3,4]	[4,6]	[5,7]	[60,168]
11	[3,4]	[4,6]	[7,7]	[84,168]
12	[3,4]	[4,6]	[7,7]	[84,168]
13	[3,4]	[5,6]	[5,7]	[75,168]
14	[3,4]	[5,6]	[7,7]	[105,168]
15	[3,4]	[5,6]	[7,7]	[105,168]
16	[3,4]	[7,7]	[5,7]	[105,196]
17	[3,4]	[7,7]	[7,7]	[147,196]
18	[3,4]	[7,7]	[7,7]	[147,196]
19	[3,3]	[4,6]	[5,7]	[60,126]
20	[3,3]	[4,6]	[7,7]	[84,126]
21	[3,3]	[4,6]	[7,7]	[84,126]
22	[3,3]	[5,6]	[5,7]	[75,126]
23	[3,3]	[5,6]	[7,7]	[105,126]
24	[3,3]	[5,6]	[7,7]	[105,126]
25	[3,3]	[7,7]	[5,7]	[105,147]
26	[3,3]	[7,7]	[7,7]	[147,147]
27	[3,3]	[7,7]	[7,7]	[147,147]

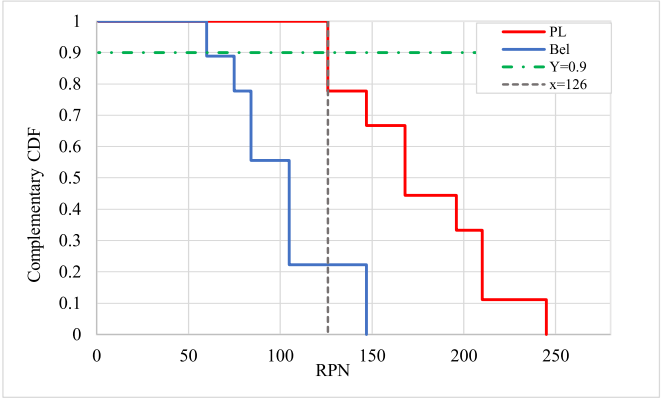

Fig. 4. Belief and Plausibility Curves belonging to failure mode 15.

two branches: one showing the consequence in case of successful action of the barrier, the other in case of failure of the safety barrier, generally causing the further development of the scenario. Table 11 reports the possible consequences arising as a result of accident occurrence, including small fire complications, environmental pollution, toxic effects, huge fire complications, etc.

3.4.2. Mapping Bow-Tie into equivalent credal network

In this stage, the representation of relationships among the variables, and the reflection of the degree of dependency between the parent node and its child node were determined. There were some dependencies between elements of the model that could not be outlined directly in the Bow-Tie approach. For instance, PE_{22} (*Structural deficiency*) is the common cause for the failure of "*Tank lid leakage*", "*Drain valve leakage*", "*Inlet and outlet valve leakage*", and "*Flange leakage*". Therefore, the Bow-Tie model was mapped into its equivalent CN following the simplified procedure shown in Fig. 7 for the AND and OR gates, respectively.

The initially created CN consists of conditional probabilities that take only binary form ("0" and "1" in the state of "success" or "failure" describe the non-occurrence and occurrence of an event, respectively). The derived binary states (0 or 1) in the CPTs for OR and AND gates make some states' outcomes deterministic. For example, as shown in Fig. 7(a), the event IE_1 (*Inappropriate inlet and outlet valve fastening*), would fail unavoidably when events PE_{34} (*Unsafe human behavior*) and PE_{35} (*Lack of valves' indicators*) are true even though the event IE_1 may not fail. Similarly, as shown in Fig. 7(b) on the success condition of both event PE_5 (*Permit's un-usage*) and event PE_6 (*Poor permit implementation*) the failure of event IE_2 (*Poor issuance system permit)* is still probable.

Table 9
Ranking of failure mode according the 90% confidence of the upper bound of RPN and associated believe function.

Failure Mode	$Bel(\overline{RPN_i^*})$	$\overline{RPN_i^*}$	Ranking
FM_{21}	0.222222	400	1
FM_{20}	0	400	2
FM_{23}	–	280	3
FM_{22}	–	256	4
FM_{16}	–	250	5
FM_5		240	6
FM_{17}	–	224	7
FM_2	–	210	8
FM_1	–	180	9
FM_{18}	–	168	10
FM_{10}	–	160	11
FM_{19}	–	135	12
FM_{15}	–	126	13
FM_{12}	–	120	14
FM_{14}	0.222222	108	15
FM_{11}	0	108	16
FM_3	0.148148	100	17
FM_4	0	100	18
FM_6	0.074074	84	19
FM_{13}	0	84	20
FM_8	–	80	21
FM_9	–	72	22
FM_7	–	63	23

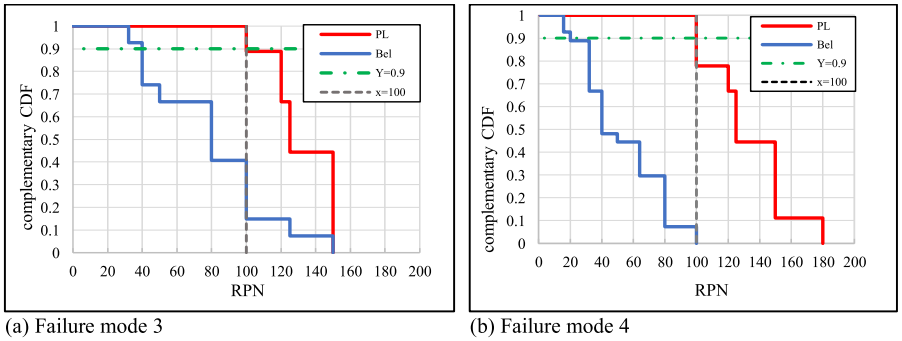

(a) Failure mode 3 (b) Failure mode 4

Fig. 5. Belief and Plausibility curves belonging to (a) FM_3 and (b) FM_4.

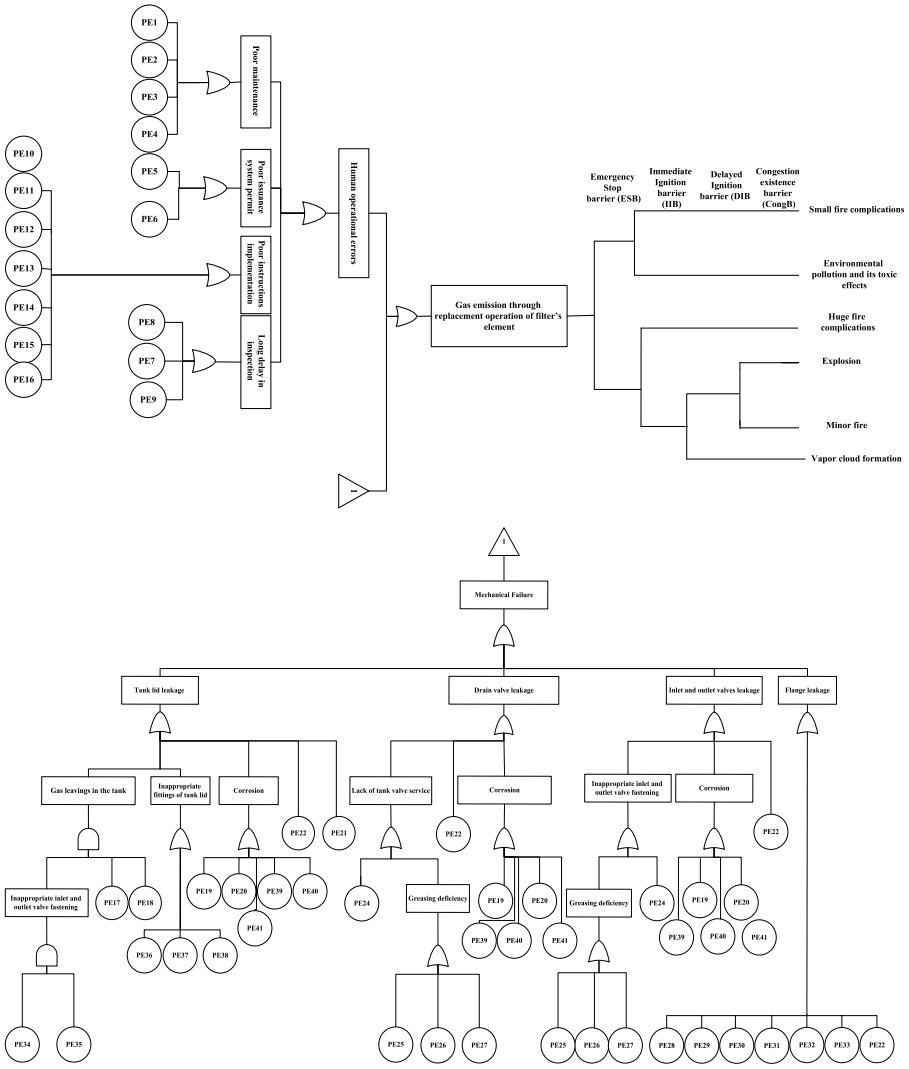

Fig. 6. Bow-Tie model for the hazard scenario identified in phase 1.

Table 12 shows the amending CPT of an AND gate for intermediate node IE_1, (*Inappropriate inlet and outlet valve fastening*) concerning the conditional probabilities of its parents. Table 13 reports the amending CPT of the OR gate of the intermediate node IE_2 (*Poor issuance system permit*) concerning the conditional probabilities of its parents. The probability λ_i was established by using tacit and explicit engineering safety knowledge from a team of experts.

The primary events of the CN must be quantified probabilistically. In the absence of data, experts expressed their perception and knowledge about the probability of the primary nodes via empirical interval-numeric values, shown in Table 14. Equal BPA was allocated to the three sources of information that $m_1 = m_2 = m_3 = 1/3$. The probability of primary events obtained from three experts, all with the same weight, is displayed in Table 14.

Belief and *Plausibility* were calculated as the Cartesian product of all masses (intervals) associated with each aggregated interval. A confidence level of 90% was used to estimate the threshold value of primary events as the critical prior probabilities. For example, in Table 15, the aggregated interval related to the primary event 32 is provided, while the corresponding Belief and Plausibility curves are illustrated in Fig. 8. The calculations revealed that the upper probability for the primary event 32, i.e., $\overline{PE_{32}}^{*}$ was determined to be $4.00{\cdot}10^{-5}$.

Furthermore, Fig. 9 displays the *Belief* and *Plausibility* curves of primary events PE_{10} (*Human negligence due to repetitive missions*), PE_{14} (*Lack of sufficient experience*), PE_{17} (*Inadequate ventilation*), PE_{19} (*Improper weather conditions*), PE_{28} (*Unstable state of the screw*), and PE_{38} (*Screw fatigue and it's cut off*). Due to space limitations, the remaining primary events are not included in this report. The evaluation of these events at a 90% confidence level reveals estimated probabilities of 0.06, 0.0099, 0.02, 0.0002, 0.0007, and 0.0001, respectively. Additionally, Table 16 displays the estimated critical probabilities for the primary events ($\overline{PE_i^*}$), and the safety barriers (S_i).

Conditional dependencies were considered for the probability of failure of safety barriers, for instance $S_{3,1} = 0.7$ shows the probability of failure of DIB in case of successful action of ESB and $S_{3,2} = 0.9$ in case of failure of ESB. The identified values for the primary event with the CPTs were used as evidence for credal inference.

Although the interval formed by the [$\underline{PE_i}$, $\overline{PE_i}$] could be used in Credal Network packages directly (Patelli et al., 2018), in this work only the upper bounds were used and therefore reducing Credal Network into a Bayesian Network. The latter was implemented in a commercial package GeNiE 2.0 softwere (GeNIe, 2019) . The Bayesian Network is shown in Fig. 10. The symbols PE and IE depict the primary and intermediate nodes, respectively; a yellow box marks the hazard scenario; and the orange and red boxes are marked as a consequence and the safety nodes, respectively. The probability of the hazard scenario occurrence was computed to be 0.1866. As well, the probabilities of eight corresponding consequences, including *Small fire complications,*

Table 10
Symbols and descriptions of Bow-Tie model's component.

Primary Event	Description	Primary Event	Description
PE_1	Unavailability of demanded equipment	PE_{25}	Valve not-turning after greasing
PE_2	Lack of timely manner of equipment demand	PE_{26}	Valve Improper state all through greasing
PE_3	Lack of sufficient expertise	PE_{27}	Irregular greasing
PE_4	Lack of equipment calibration	PE_{28}	Unstable state of the screw
PE_5	Permit's un-usage	PE_{29}	Washer improper installation
PE_6	Poor permit implementation	PE_{30}	Washer fatigue
PE_7	Deficiency in leak diagnosis	PE_{31}	Overpressure on the washer
PE_8	Lack of leak diagnosis confirmation	PE_{32}	Screw head cut off
PE_9	Irregular thickness inspection on the filter and its facilities	PE_{33}	Insufficient tightening force on the screw
PE_{10}	Human negligence due to repetitive missions	PE_{34}	Unsafe human's behavior
PE_{11}	Non-standard equipment	PE_{35}	Lack of valves' indicators
PE_{12}	Unpredictable gas interruption of subscribers	PE_{36}	Unclenched state of moving screws
PE_{13}	Hastiness and stress during work	PE_{37}	Holding the retaining screws ON.
PE_{14}	Lack of sufficient experience	P_{38}	Screw's fatigue and its cut off
PE_{15}	Lack of sufficient training	PE_{39}	Poor inspection of corrosion
PE_{16}	Wrong risk assessment	PE_{40}	Erosion
PE_{17}	Inadequate ventilation	PE_{41}	Non-standard fluid velocity
PE_{18}	Blockage state of the safety lock	S_1	Emergency Shutdown barrier (ESB)
PE_{19}	Improper weather conditions	S_2	Immediate ignition barrier (IIB)
PE_{20}	Anti-corrosion coating's failure	S_{31}	Delayed ignition barrier (DIB) when ESB worked
PE_{21}	O-Ring's fatigue	S_{32}	Delayed ignition barrier (DIB) when ESB failed
PE_{22}	Structural deficiency	S_4	Congestion existence (Cong)
PE_{24}	Valve fatigue and its cut off		

Table 11
Output event consequences of the Bow-Tie model.

Consequences	Description
C_1	Small fire complications
C_2	Environmental pollution and toxic effects
C_3	Huge fire complications
C_4	Minor fire
C_5	Explosion
C_6	Vapor cloud formation
C_7	Safety state

Environmental pollution, Vast fire complications, Explosion, Minor fire, and Vapor cloud formation, were estimated to be 0.0168, 0.0392, 0.0392, 0.0576, 0.0247, and 0.0091, respectively.

Bayesian (Credal) Networks enable diagnostic analysis, allowing for reasoning from symptoms to causes. This implies that, based on the system's condition, one can obtain the posterior probability distribution for the primary event (Yazdi et al., 2021). For instance, the observation of hazard scenario occurrence corresponding to FM_{21} (i.e., *Gas emission through replacement operation of filter's element)* and consequence C_4 (i.e., *Explosion)* can serve as new evidence, leading to the updating of prior probabilities for all primary and safety nodes. The findings of this diagnostic analysis are presented in Table 17.

By comparing the prior probabilities with the updated probabilities

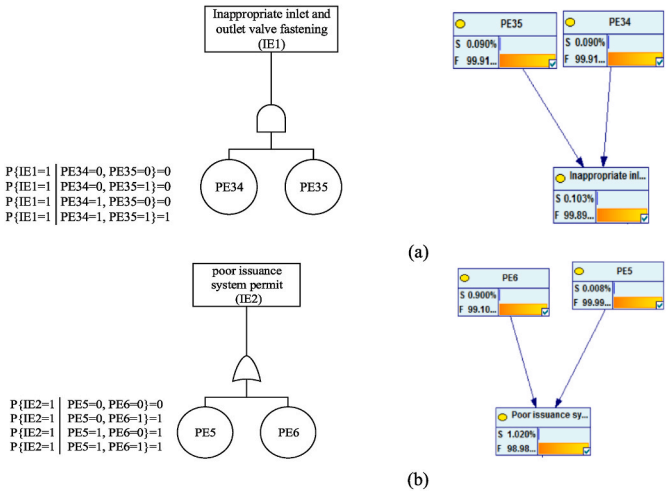

Fig. 7. Conversion rules between logic gates of Bow-Tie into its corresponding Credal Network: (a) for the AND gate, (b) for OR gate.

Table 12
Amending CPTs of "AND" gate for $\boldsymbol{E_1}$.

PE34		Success		Failure	
PE35		Success	Failure	Success	Failure
IE1	**Success**	0.98	0.02	0.02	0.001
	Failure	0.02	0.98	0.98	0.999

Table 13
Amending CPTs of "OR" gate foe $\boldsymbol{IE_2}$.

PE5		Success		Failure	
PE6		Success	Failure	Success	Failure
IE2	**Success**	0.98	0.96	0.96	0.0015
	Failure	0.02	0.04	0.04	0.9985

of primary events, critical primary events can be pinpointed as those with a substantial increase in probability and a high posterior probability.

By considering the occurrence of the hazard scenario, the prior probabilities were compared with the posterior probabilities of primary events and the result is shown in Fig. 11.

Clearly, PE_{10}, PE_6, PE_3, PE_{17}, PE_{22}, PE_{36}, and PE_{13} show a substantial increase in the posterior probability values with respect their prior values.

Of these, the primary event PE_{10} (*Human negligence due to repetitive missions)* stands out as the most influential contributor to the hazard scenario probability, earning its rank as the most critical component. Following closely are PE_6 (*Poor permit implementation)*, PE_3 (*Lack of sufficient expertise*), PE_{17} (*Inadequate ventilation)*, PE_{22} (*Structural deficiency)*, PE_{36} (*Unclenched state of moving screws),* and PE_{13} (*Hastiness and stress and during work)*, which also play vital roles in the occurrence of "Gas emission through replacement operation of filter's element. Therefore, these events contribute to top event occurrence, and closer attention must be paid to these events to prevent the hazard scenario occurrence.

The results also follow the research that has underscored the human factors' role in chemical process industries (Milazzo et al., 2021; Morais et al., 2019; Polavarapu, 2021; Qiao et al., 2020).

3.4.3. Sensitivity analysis

In this work, SA was used to appoint the probability of a specified target node to individual primary events. To this end, prior probability

Table 14
Experts' knowledge of the primary events' probabilities.

Primary Event	Expert 1	Expert 2	Expert 3
PE_1	[1.00E-3, 1.20E-3]	[5.00E-4, 1.00E-3]	[5.00E-4, 1.50E-3]
PE_2	[1.50E-3, 2.00E-3]	[5.00E-4, 1.50E-3]	[5.00E-4, 1.00E-3]
PE_3	[2.50E-3, 3.00E-3]	[2.50E-3, 3.00E-3]	[1.50E-3, 2.00E-3]
PE_4	[1.50E-3, 2.00E-3]	[1.50E-3, 2.50E-3]	[1.00E-3, 1.80E-3]
PE_5	[2.00E-7, 3.00E-7]	[5.00E-7, 1.00E-6]	[8.00E-7, 3.00E-6]
PE_6	[1.50E-2, 2.00E-2]	[1.00E-2, 1.20E-2]	[2.00E-2, 2.30E-2]
PE_7	[8.00E-6, 1.50E-5]	[5.00E-6, 1.00E-5]	[5.00E-6, 1.50E-5]
PE_8	[5.00E-5, 9.00E-5]	[4.00E-5, 6.00E-5]	[4.00E-5, 6.00E-5]
PE_9	[1.00E-3, 1.50E-3]	[1.00E-3, 1.50E-3]	[5.00E-4, 1.00E-3]
PE_{10}	[3.50E-2, 4.00E-2]	[2.00E-2, 3.50E-2]	[3.50E-2, 4.00E-2]
PE_{11}	[1.50E-3, 2.00E-3]	[1.50E-3, 2.00E-3]	[1.00E-3, 1.20E-3]
PE_{12}	[5.00E-6, 8.00E-6]	[6.00E-6, 9.00E-6]	[3.00E-6, 7.00E-6]
PE_{13}	[2.00E-3, 3.00E-3]	[1.50E-3, 2.00E-3]	[2.50E-3, 3.00E-3]
PE_{14}	[2.00E-3, 2.50E-3]	[1.50E-3, 2.00E-3]	[2.00E-3, 2.50E-3]
PE_{15}	[1.00E-3, 1.50E-3]	[1.00E-3, 1.50E-3]	[1.50E-3, 2.00E-3]
PE_{16}	[1.00E-6, 3.00E-6]	[2.00E-6, 3.00E-6]	[8.00E-6, 9.90E-6]
PE_{17}	[8.00E-5, 9.90E-5]	[7.00E-5, 8.00E-5]	[5.00E-5, 6.00E-5]
PE_{18}	[5.00E-6, 9.00E-6]	[5.00E-6, 9.00E-6]	[8.80E-6, 1.00E-5]
PE_{19}	[1.00E-4, 1.50E-4]	[1.00E-4, 1.20E-4]	[1.50E-4, 2.00E-4]
PE_{20}	[3.00E-4, 9.00E-4]	[4.00E-4, 6.00E-4]	[3.00E-4, 8.00E-4]
PE_{21}	[8.00E-5, 9.00E-5]	[8.80E-5, 9.90E-5]	[7.00E-5, 9.03E-5]
PE_{22}	[4.00E-4, 9.00E-4]	[4.00E-4, 5.00E-4]	[5.00E-4, 9.00E-3]
PE_{24}	[5.00E-6, 8.00E-6]	[5.00E-6, 8.00E-6]	[3.00E-6, 6.00E-6]
PE_{25}	[5.00E-2, 1.50E-1]	[8.00E-3, 1.50E-2]	[1.00E-1, 2.00E-1]
PE_{26}	[2.00E-3, 3.00E-3]	[5.00E-4, 1.50E-3]	[1.50E-3, 2.00E-3]
PE_{27}	[1.50E-4, 2.00E-4]	[5.00E-4, 1.50E-3]	[5.00E-4, 1.00E-3]
PE_{28}	[5.00E-4, 8.00E-4]	[4.00E-4, 7.00E-4]	[8.00E-4, 1.00E-3]
PE_{29}	[7.00E-6, 9.00E-6]	[7.00E-6, 9.00E-6]	[5.00E-6, 9.00E-6]
PE_{30}	[9.00E-5, 4.00E-4]	[3.00E-4, 5.00E-4]	[3.00E-4, 5.00E-4]
PE_{31}	[3.00E-4, 5.00E-4]	[5.00E-4, 9.00E-4]	[2.00E-4, 6.00E-4]
PE_{32}	[1.00E-5, 4.00E-5]	[3.00E-5, 5.00E-5]	[2.00E-5, 6.00E-5]
PE_{33}	[4.00E-6, 7.70E-6]	[5.00E-6, 7.00E-6]	[9.90E-6, 1.00E-5]
PE_{34}	[5.00E-4, 1.00E-3]	[1.00E-3, 1.20E-3]	[5.00E-4, 1.50E-3]
PE_{35}	[5.00E-4, 9.00E-4]	[5.00E-4, 4.00E-4]	[8.80E-5, 1.00E-4]
PE_{36}	[1.00E-6, 3.00E-6]	[4.00E-7, 5.00E-7]	[1.00E-6, 3.00E-6]
PE_{37}	[1.00E-7, 2.00E-7]	[1.00E-7, 2.00E-7]	[4.00E-7, 5.00E-7]
PE_{38}	[4.00E-6, 5.00E-6]	[1.00E-6, 5.00E-6]	[4.40E-6, 6.00E-6]
PE_{39}	[7.00E-6, 9.00E-6]	[3.00E-6, 5.00E-6]	[4.00E-6, 8.00E-6]
PE_{40}	[1.50E-3, 2.00E-3]	[1.50E-3, 2.00E-3]	[1.20E-3, 2.50E-3]
PE_{41}	[5.00E-5, 7.00E-5]	[7.00E-5, 8.00E-5]	[2.00E-5, 3.00E-5]

Table 15
All possible combinations of PE_{32}.

Combination Number	Interval
1	[1.00E-5,4.00E-2]
2	[1.00E-5,5.00E-5]
3	[1.00E-5,6.00E-5]
4	[3.00E-5, 4.00E-2]
5	[3.00E-5, 5.00E-5]
6	[3.00E-5, 6.00E-5]
7	[2.00E-5, 4.00E-2]
8	[2.00E-5, 5.00E-5]
9	[2.00E-5, 6.00E-5]

values of identified critical primary events were subjected to a change of ± 10% and the target node was FM_{21}. The results of the SA are shown in Table 18.

When the probability of PE_{10} was subjected to an increase of 10%, the probability of hazard scenario incidence increased from 18.66% to 19.02%. When probabilities of both PE_{10} *and* PE_6 were increased by 10%, the probability of hazard scenario occurrence increased from 19.02% to 19.08%. When probabilities of PE_{10}, PE_6, and PE_3 were increased by 10%, the probability of undesired event occurrence changed from 19.08% to 19.14%. When the probabilities of PE_{10}, PE_6, PE_3, and PE_{17} were increased by 10%, the probability of undesired event occurrence increased from 19.14% to 19.20%. When the probabilities of PE_{10}, PE_6, PE_3, PE_{17}, and P_{22} were increased by 10%, simultaneously the probability of hazard scenario occurrence increased from 19.20% to

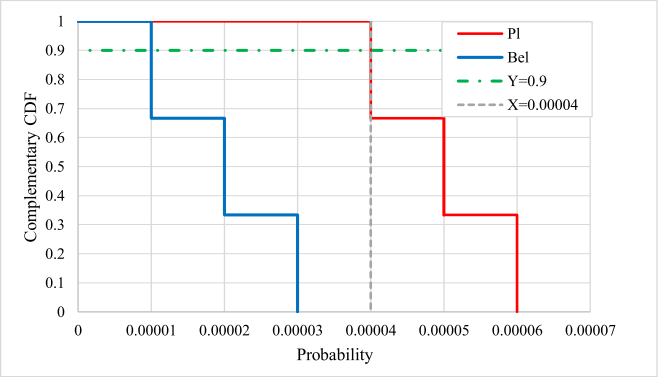

Fig. 8. Belief and Plausibility curves belonging to PE_{32}.

19.24%. When the probabilities of PE_{10}, PE_6, PE_3, PE_{17}, PE_{22}, and PE_{36} were increased by 10%, the probability of hazard scenario occurrence increased from 19.24% to 19.26%. When the probabilities of PE_{10}, PE_6, PE_3, PE_{17}, PE_{22}, PE_{36}, and PE_{13} were increased by 10%, simultaneously the probability of hazard scenario occurrence increased from 19.24% to 19.28%. Similarly, the decrease of primary events' probabilities produces a decrease in the probability of occurrence of worst-case hazard scenario in the same way as shown in Fig. 12.

The results of the SA performed in this study satisfied the three axioms set by Jones (Jones et al., 2010). Therefore, the proposed model is partially verified since a slight change in the probabilities of primary events led to a reasonable variation in the occurrence probability of the selected target, FM_{21}. Maintaining consistency with diagnostic analysis results as the descending order of contributing factors remained the same in posterior probability analysis.

3.5. Phase 3: risk mitigation

Once failure modes, the hazard scenario, and contributing factors have been identified, mitigation measures can be suggested to reduce the likelihood and consequences of these failures, i.e., reducing the associated risk. In this phase, it is essential to involve key stakeholders in the risk mitigation process to gather diverse perspectives and insights. This can help ensure that all relevant consequences are identified and that appropriate mitigation measures are suggested. The mitigation measures should be specific, actionable, and tailored to address the identified risks effectively. Additionally, regular review and updating of risk analysis is necessary to adapt to changing circumstances and new risks that may arise.

Following the two previous phases, the most contributing factor leading to the hazard scenario identified was "Human negligence due to repetitive missions". Some action plans are proposed to address this factor, reduce its likelihood and impact.

Human negligence due to repetitive missions: 1) utilizing automation and technology solutions to streamline repetitive tasks and reduce the potential for human error due to negligence can be beneficial. This includes using software tools for data entry, scheduling reminders for critical tasks, or deploying sensors for monitoring equipment performance. **2)** regular safety checks and audits should be implemented on a strict schedule to ensure that all protocols and procedures are being followed correctly, helping identify any potential areas of negligence and addressing them promptly to prevent accidents or errors. **3)** creating safety within the organization, where employees are encouraged to report errors or near misses without fear of reprisal, promotes transparency and accountability, aiding in the identification and prevention of negligence from recurring. **4)** establishing performance metrics and key performance indicators (KPIs) related to job duties and responsibilities can effectively track employee performance, helping identify any deviations or trends indicative of negligence through

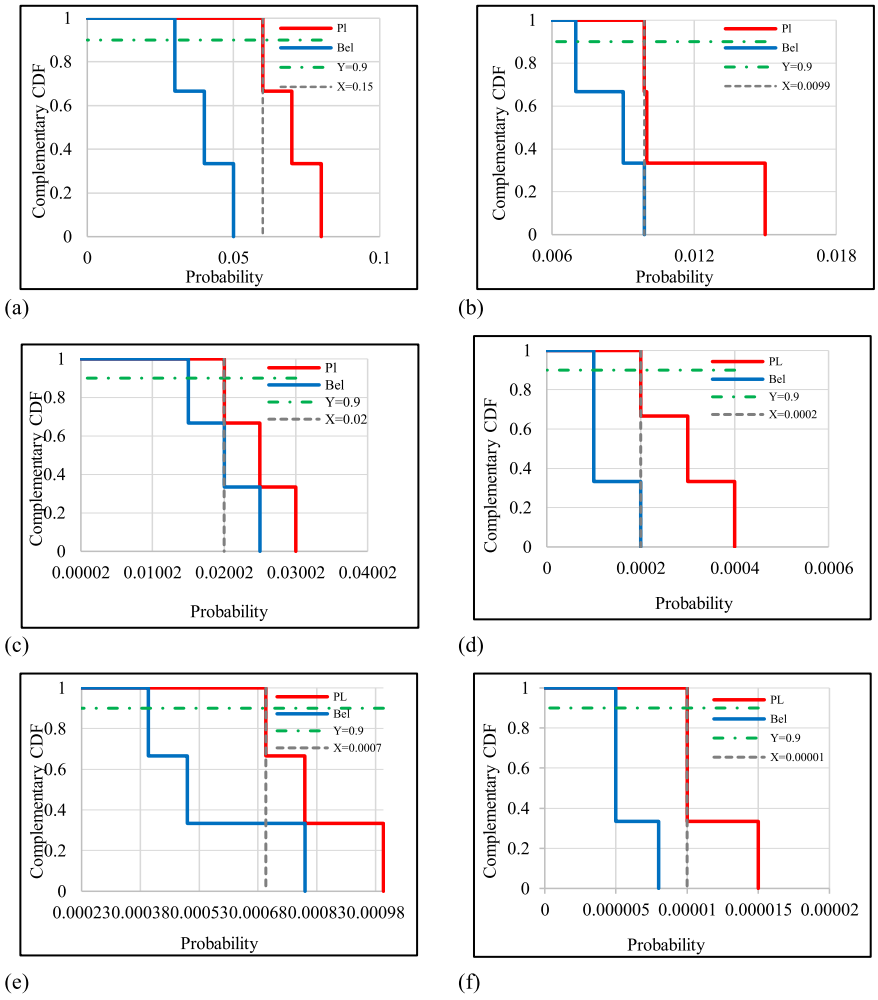

Fig. 9. Belief and Plausibility curves belonging to PE_{10} (a), PE_{14} (b), PE_{17} (c), PE_{19} (d), PE_{28} (e), PE_{38} (f).

Table 16
Estimated primary events' prior probabilities.

Primary Event	Prior probability	Primary Event	Prior probability
PE_1	1.00E-3	PE_{25}	2.00E-3
PE_2	1.00E-3	PE_{26}	2.00E-3
PE_3	9.00E-3	PE_{27}	1.50E-3
PE_4	1.80E-3	PE_{28}	7.00E-4
PE_5	8.00E-5	PE_{29}	1.00E-5
PE_6	9.0E-3	PE_{30}	4.00E-4
PE_7	1.00E-5	PE_{31}	5.00E-4
PE_8	6.00E-5	PE_{32}	4.00E-5
PE_9	1.00E-3	PE_{33}	1.00E-5
PE_{10}	6.00E-2	PE_{34}	9.00E-4
PE_{11}	9.00E-3	PE_{35}	9.00E-4
PE_{12}	9.00E-5	PE_{36}	1.00E-3
PE_{13}	9.90E-3	PE_{37}	1.00E-5
PE_{14}	9.90E-3	P_{38}	1.00E-5
PE_{15}	9.93E-3	PE_{39}	1.00E-5
PE_{16}	1.00E-4	PE_{40}	5.00E-3
PE_{17}	2.00E-2	PE_{41}	9.00E-4
PE_{18}	4.00E-3	**Safety event**	
PE_{19}	2.00E-4	S_1	2.70E-1
PE_{20}	6.00E-4	S_2	3.90E-1
PE_{21}	1.00E-5	$S_{3,1}$	7.00E-1
PE_{22}	9.00E-3	$S_{3,2}$	9.00E-1
PE_{24}	1.00E-5	S_4	7.00E-1

regular reviews. **5)** a job rotation program should be developed to offer employees diverse experiences and prevent them from becoming too complacent in their current roles by moving employees through different roles and responsibilities within the organization. This can help prevent employees from becoming stagnant in their current roles, keeping them engaged and motivated. **6)** clear reporting and investigation protocols should be implemented for employees to report incidents, near misses, or concerns related to negligence. By creating a structured process for reporting and investigating incidents, organizations can address issues promptly, identify root causes, and implement corrective actions to prevent recurrence. **7)** involving employees in safety committees, task forces, or safety improvement initiatives to empower them to contribute ideas, identify risks, and propose solutions to prevent negligence. By engaging employees in safety initiatives, organizations can leverage their insights and experiences to enhance safety practices and prevent incidents of negligence. **8)** offer access to employee assistance programs (EAPs) to support employees' mental health, well-being, and work-life balance. By addressing employees' stress, fatigue, and personal challenges, organizations can prevent distractions, errors, and instances of negligence stemming from personal issues impacting work performance.

Once appropriate mitigation measures are defined, they need to be implemented within the CGS system. It is crucial to have a system in place to track the progress of the mitigation measures, monitor their impact, and subsequently make adjustments as necessary. Continuous monitoring and review, including regular risk assessments, internal

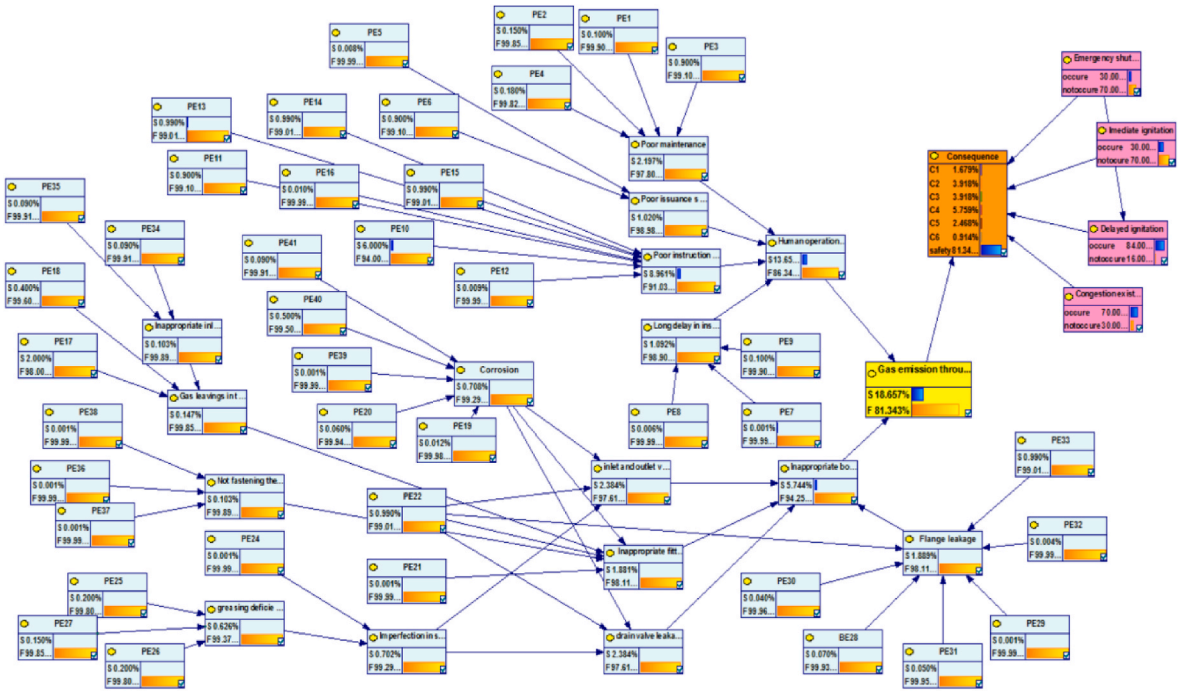

Fig. 10. Bayesian network derived and defined in GeNie software.

Table 17
Primary events' posterior probabilities.

Primary event	Posterior probability	Primary event	Posterior probability
PE_1	4.40E-3	PE_{25}	9.20E-3
PE_2	6.70E-3	PE_{26}	9.20E-3
PE_3	4.02E-2	PE_{27}	6.90E-3
PE_4	8.00E-3	PE_{28}	2.90E-3
PE_5	3.00E-4	PE_{29}	4.00E-5
PE_6	4.16E-2	PE_{30}	1.60E-3
PE_7	4.00E-5	PE_{31}	2.00E-3
PE_8	2.00E-4	PE_{32}	1.00E-4
PE_9	4.60E-3	PE_{33}	4.18E-2
PE_{10}	2.46E-1	PE_{34}	9.00E-4
PE_{11}	3.69E-2	PE_{35}	9.00E-4
PE_{12}	3.00E-4	PE_{36}	4.30E-3
PE_{13}	4.06E-2	PE_{37}	4.00E-5
PE_{14}	4.06E-2	P_{38}	4.00E-5
PE_{15}	4.06E-2	PE_{39}	4.00E-5
PE_{16}	4.00E-4	PE_{40}	2.32E-2
PE_{17}	2.12E-2	PE_{41}	4.10E-3
PE_{18}	4.20E-3	**Safety event**	
PE_{19}	5.00E-4	S_1	3.30E-1
PE_{20}	2.70E-3	S_2	4.70E-1
PE_{21}	4.00E-5	S_{31}	1
PE_{22}	4.98E-2	S_{32}	1
PE_{24}	4.00E-5	S_4	1

audits, and external reviews, are essential aspects of the risk analysis and mitigation process. They help assess the performance of existing mitigation measures and ensure that the risk management processes remain robust and adaptive. This aspect can be analyzed in future studies as the fourth phase of the risk management of the current study. This study does not quantify the impact of suggested measures but only suggests some potential mitigation strategies. The results of this part may provide some insight for policy-makers to formulate and execute the suggested policies and prevention strategies.

4. Discussion and limitations of the approach

The present study employs a highly practical yet robust approach to assessing risks by incorporating three phases, including risk identification, analysis, and mitigation. The proposed approach is based on industrial standard techniques such as FMECA, Bowtie, and Credal Network, coupled with robust modeling of uncertainty based on D-S theory. The approach is generally applicable and especially important when there is no exact evidence introduced in the analysis, ambiguities arise from different sources of information, or when there is not enough information. This provides a more reliable risk assessment process compared to some quantitative methodologies that may struggle to deal with conflicting data types and uncertainty. The approach also allows one to select the level of confidence desired (to define the probability of the events) and to understand the need and consequences of collecting more data to improve the knowledge about specific factors.

Nevertheless, it is crucial to acknowledge the limitations and challenges inherent in the developed approach. The proposed approach makes use of multiple methods that can lead to prolonged assessment processes, potentially challenging industries with tight timelines. Moreover, the interpretation of the results may require more specialized skills for effective analysis. Additionally, the approach introduces some computational complexity, particularly with a large number of hypotheses considered, which hinders communication with non-technical audiences. However, this limitation can be alleviated by providing training for effective result interpretation, which can bridge the gap between technical and non-technical audiences.

The constructed Bow-Tie model relies on the expertise of the involved experts. As a result, it is uncertain whether all relevant factors of the model were considered by the experts in a real decision-making context or if their hypothetical decisions would accurately reflect real-world actions. Neglecting other relevant factors that could be relevant to the hazard scenario of CGS could result in an incomplete understanding of the overall risk profile of the station. Thus, a necessary course of action can be taken by implementing a structured validation process, such as peer reviews and expert panels, which can help ensure the accuracy and completeness of the Bow-Tie model.

It is crucial to acknowledge that risk management extends beyond the three phases presented here. For instance, in phase 3 some mitigation measures were suggested to address the identified risks, but the feasibility and sustainability of the proposed solutions have not been

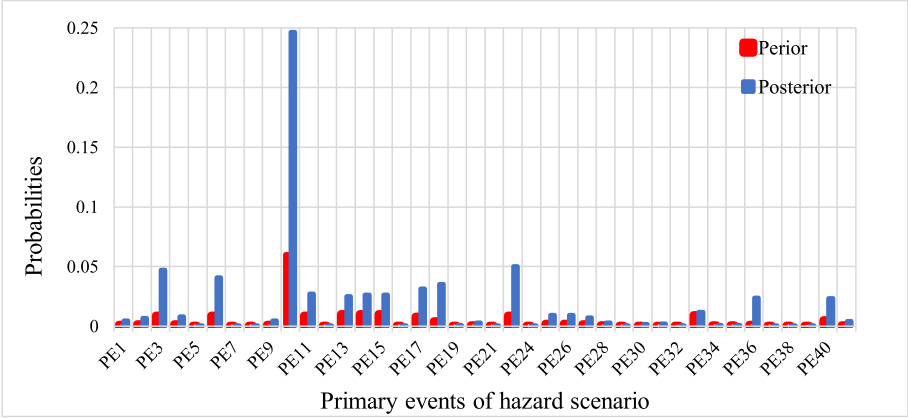

Fig. 11. Comparison of probability changes in primary events following the hazard scenario occurrence.

Table 18
Sensitivity values of contributing factors on probability of hazard scenario occurrence.

Critical primary nodes	D(SA)
PE_{10}	1.019721
PE_{10}, PE_6	1.02299
PE_{10}, PE_6, PE_3	1.026152
PE_{10}, PE_6, PE_3, PE_{17}	1.029046
PE_{10}, PE_6, PE_3, PE_{17}, PE_{22}	1.03119
PE_{10}, PE_6, PE_3, PE_{17}, PE_{22}, PE_{36}	1.032315
PE_{10}, PE_6, PE_3, PE_{17}, P_{22}, PE_{36} , PE_{13}	1.033387

analyzed. Exploring alternative preventive measures can lead to the identification of innovative solutions that may not have been considered initially. This encourages a more comprehensive and strategic view to risk mitigation, ensuring that industries have access to a diverse set of tools and strategies to manage risks effectively.

5. Conclusions

In this paper, a systematic accident scenario of a City Gate Station which is one of the most vital installations of gas transferring networks was developed. The proposed methodology offers a comprehensive and structured approach for risk assessment of high-risk process industries under uncertainty, especially for complex systems with limited, contradictory, or conflicting information by incorporating phases of risk identification, analysis, and mitigation, leading to effective risk management strategies. Utilizing multiple methods like FMECA, Bow-Tie, Credal Network, and D-S theory, the methodology ensures a thorough analysis of risks and the integration of mitigation strategies for proactive risk reduction.

The approach utilized *Belief* and *Plausibility* curves to facilitate the propagation of uncertainty. By doing so, it effectively addresses the epistemic uncertainty inherent in experts' risk factor ratings, allowing for interval-valued analysis and providing a more comprehensive representation of experts' knowledge and perception. It also eliminates the need for experts to express a belief probability assignment and avoids assumptions about the distribution of BPAs, enabling the handling of conflicting judgments. Moreover, the uncertainty of the input data is appropriately propagated throughout the analysis, maintaining an epistemic approach until the final results are obtained. By considering uncertainty and imprecise information in risk assessment, policymakers can develop more robust regulations and standards that promote a culture of safety, transparency, and accountability within the industry. This can lead to improved safety standards, enhanced emergency response protocols, and a more resilient infrastructure that safeguards the well-being of both workers and the surrounding community.

The case study conducted a thorough analysis of the City Gate Station and identified the most critical failure mode as the "*Gas emission*

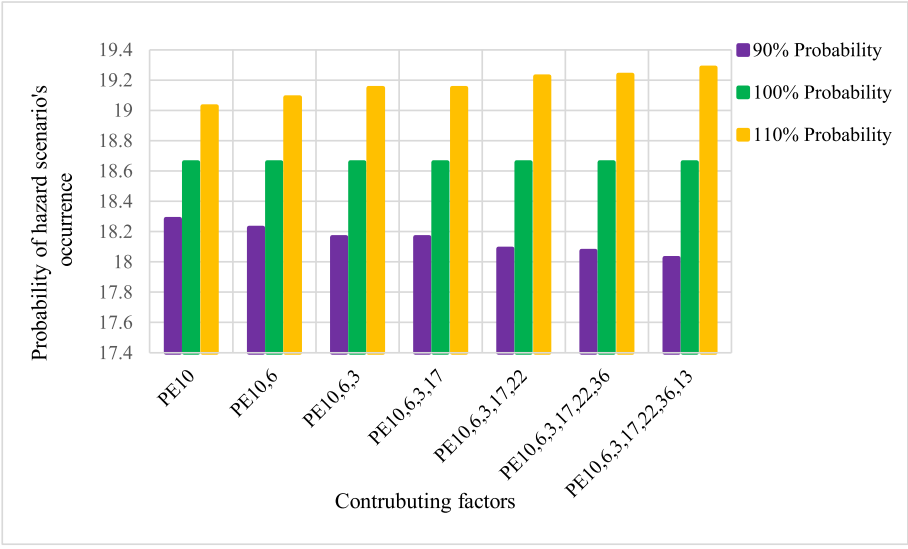

Fig. 12. Sensitivity analysis of contributing factors on probability of hazard scenario occurrence.

through filter replacement operation" through the FMECA process, while considering expert imprecision. This worst-case hazard scenario was then modeled using the Bow-Tie method and mapped into a Credal Network to quantify the risk and to provide a detailed understanding of the root cause and key contributing factors such as "*Human negligence due to repetitive missions*", "*Poor permit implementation*", "*Lack of sufficient expertise*", "*Inadequate ventilation*", "*Structural deficiency*", "*Unclenched state of moving screws*", and "*Hastiness and stress and during work*". Recommendations were provided to address identified contributing factors to reduce the likelihood of accidents at City Gate Stations and enhance overall safety performance and reliability. Implementing these interventions can proactively manage risks, improve safety performance, and create a secure operational environment at the stations.

These results highlight the significance of employing advanced analytical techniques in identifying, analyzing, and mitigating risks in complex systems. Although the approach proposed has been applied to a City Gate Stations, it can be adopted in other engineering fields or safety cases where often probabilities are estimated from limited data or expert elicitation.

CRediT authorship contribution statement

Batool Rafiee: Writing – review & editing, Writing – original draft, Validation, Software, Methodology, Investigation, Formal analysis, Data curation, Conceptualization. **Davood Shishebori:** Writing – review & editing, Validation, Supervision, Funding acquisition. **Edoardo Patelli:** Writing – review & editing, Validation, Supervision, Methodology.

Declaration of competing interest

The authors declare the following financial interests/personal relationships, which may be considered as potential competing interests: Batool Rafiee, Davood Shishebori report financial support was provided by Yazd University Faculty of Science in iran. If there are other authors, they declare that they have no known competing financial interests or personal relationships that could have appeared to influence the work reported in this paper.

Acknowledgments

This work was financially supported by the University of Yazd, Yazd, Iran (under Grant No. 83-288). The authors gratefully acknowledge the National Iranian Gas Company- Yazd province for their assistance and plausible support of this research.

Appendix A. Material and method

A.1. Dempster-Shafer theory of evidence

Dempster-Shafer (D-S) theory, was introduced by Dempster and Shafer for dealing with data inadequacy (Dempster, 1967; Shafer, 1976). D-S theory resembles a discrete probability theory except that the locations at which the probability mass resides are defined as sets of real values named as focal elements, rather than precise points. Typically, focal elements are chosen among closed intervals so-called focal intervals. In the context of expert elicitation, D-S allows expressing the beliefs in an uncertain parameter x within a certain set of intervals A and with an associated level of confidence. Mathematically, the value of x is quantified by the Basic Probability Assignment (BPA) that satisfies the following conditions:

$$0 \le m(X_i) \le 1 \tag{A.1}$$

$$m(\varnothing) = 0 \tag{A.2}$$

$$\sum_{A \in U} m(X) = 1 \tag{A.3}$$

Equation (A.1) expresses that the degree of belief m associated with each value in set X_i must be in the range of [0,1]; equation (A.2) means that no belief should be allocated to events that cannot occur; equation (A.3) expresses that the total mass (all beliefs) of X must sum to 1. The D-S variables can be plotted by drawing rectangles in which the height represents the mass m_i and the width the range X_i showing the amount of evidence cumulatively supporting the bounded ranges, The D-S structure is a set of pairs comprising closed intervals and corresponding BPAs as presented by Ferson et al. (Ferson et al., 2003a):

$$\{([a_1, b_1], m_1), ([a_2, b_2], m_2), \ldots, ([a_n, b_n], m_n)\} \tag{A.4}$$

where $a_i \le b_i \ \forall\, 1 \le i \le n$ represent the bounds of each BPA.

These intervals produce an upper and lower cumulative distribution functions known as *Belief* and *Plausibility* function (see fig. A.1).

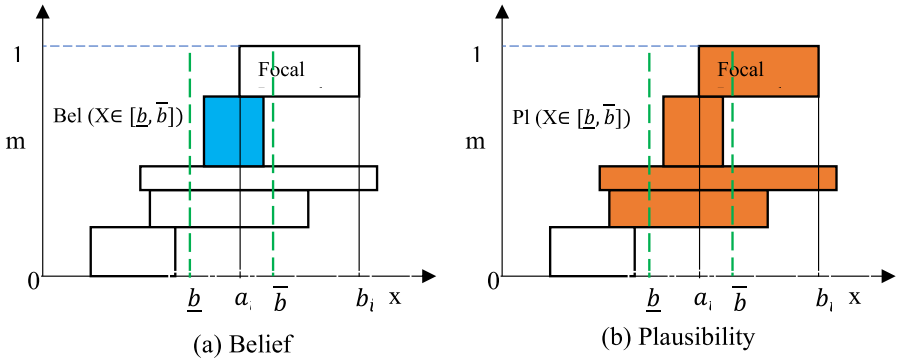

Fig. A.1. BPA of five focal and corresponding *Belief* and *Plausibility* Functions.

The *Belief* function $Bel(X \in [\underline{b}, \overline{b}])$ is formed by those focal intervals $[a_i, b_i]$ completely contained within $[\underline{b}, \overline{b}]$. On the other hand, the *Plausibility* function $Pl(X \in [\underline{b}, \overline{b}])$ is computed by considering all the focal intervals that intersect $[\underline{b}, \overline{b}]$. Therefore, given all the evidence, the *Belief* and *Plausibility* functions represent the best and worst-case scenarios, respectively (Shenoy, 2023). These two scenarios are represented by the cumulative belief and plausibility functions:

$$\underline{F}(x) = Bel(X \in (-\infty, X])) = \sum_{b_i \le x, i=1}^{n} m([a_i, b_i]) \tag{A.5}$$

$$\overline{F}(x) = Pl\,(X \in (-\infty, x])) = \sum_{a_i \le x, i=1}^{n} m([a_i, b_i]) \tag{A.6}$$

The pair of lower and upper cumulative distribution functions $[\underline{F}, \overline{F}]$ forms the so-called probability boxes or P-boxes. When the focal elements are reduced to precise values, the *Belief* and *Plausibility* functions coincide, and they represent the cumulative distribution function (CDF) of probability theory. Therefore, the probability boxes can be seen as the uncertainty around the CDF: $\underline{F}(x) \le F(x) \le \overline{F}(x)$ due to the incertitude on the BPA as can be seen in fig. A.2. The wider the distance between the upper and the lower bound is, the higher the incertitude associated with the random variable X.

Inversely, since a unique p-box, $[\underline{F}, \overline{F}]$, can induce many D-S structures, in practice a D-S structure is often approximately obtained using discretization techniques (Ferson et al., 2003b).

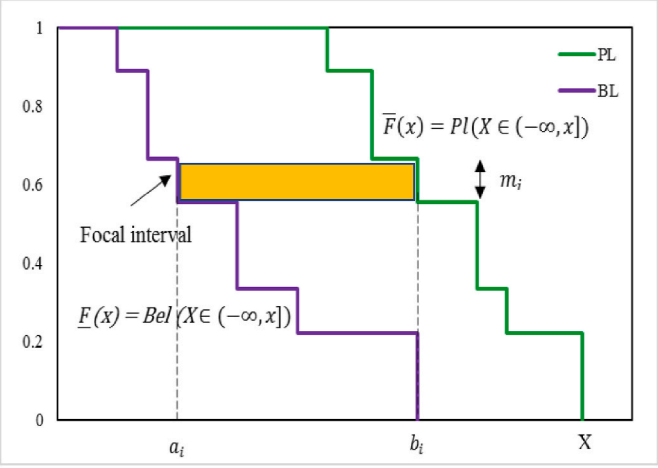

Fig. A.2. Complementary Cumulative Belief and Plausibility Functions.

A.2. Bayesian networks

A Bayesian Network (BN) is a directed acyclic graph that captures the dependencies among events via joint probability distributions. BNs provide predictive and diagnostic inference. A BN is formed by *nodes* that represent variables with parent nodes representing independent variables with assigned probability distribution functions, while child nodes depend on the status of parent nodes. *Arcs* show the dependencies among variables (i.e., they connect parents and child nodes), Conditional Probability Tables represent a unique probability distribution for every variable conditional on any configuration of the parents.

The BN can be regarded as a joint probability mass function over a collection of random variables, structured as a vector $X = (X_1, X_2, \ldots, X_n)$. Considering $pa(X_i)$ the state X_i of the *parent* node and thanks to the Markov condition (i.e., independence of each node of its non-descendant conditional on its parents) and conditional dependencies of variables, the joint probability distribution, i.e., $P(X)$ belongs to a set of variables $X = (X_1, X_2, \ldots, X_n)$ is demonstrated by (Jensen, 2001):

$$P(X) = \prod_{i=1}^{n} P(x_i | pa(X_i)) \tag{A.7}$$

Accordingly, by calculating the prior probability of variables X_i predictive reasoning can be carried out as

$$P(x_i) = \sum_{X \setminus x_i} P(X) \tag{A.8}$$

Also, once new information or pieces of evidence are available, diagnostic inference can be performed via probability updating , Hassan et al., 2022. By introducing evidence $X_E = x_E$, the updated probability of queried variable X_q, is:

$$P(x_q | x_E) = \frac{\sum_{x_M} \prod_{i=1}^{n} P(x_i | pa(X_i))}{\sum_{x_M, x_q} \prod_{i=1}^{n} P(x_i | pa(X_i))} \tag{A.9}$$

Where $X_M := X / (\{X_q\} \cup X_E)$, the domains of the arguments of the sums are left implicit and the values of X_i and $pa(X_i)_i$ are those consistent with $X = (X_q, X_M, X_E)$ (Antonucci et al., 2010).

References

Angelis, M. de, Estrada-Lugo, H.D., Patelli, E., Ferson, S., 2019. On the dimensionality of credal networks with interval probabilities. In: ISIPTA. https://doi.org/10.13140/RG.2.2.20282.75208.

Antonucci, A., Sun, Y., De Campos, C.P., Zaffalon, M., 2010. Generalized loopy 2U: a new algorithm for approximate inference in credal networks. Int. J. Approx. Reason. 51, 474–484. https://doi.org/10.1016/j.ijar.2010.01.007.

Arabkoohsar, A., Machado, L., Koury, R.N.N., 2016. Operation analysis of a photovoltaic plant integrated with a compressed air energy storage system and a city gate station. Energy 98, 78–91. https://doi.org/10.1016/j.energy.2016.01.023.

Arya, A.K., Katiyar, R., Senthil Kumar, P., Kapoor, A., Pal, D.B., Rangasamy, G., 2023. A multi-objective model for optimizing hydrogen injected-high pressure natural gas pipeline networks. Int. J. Hydrogen Energy 48, 29699–29723. https://doi.org/10.1016/J.IJHYDENE.2023.04.133.

Aslett, L.J.M., Coolen, F.P.A., 2022. Uncertainty in Engineering: Introduction to Methods and Applications. Springer. ISBN: 978-3-030-83639-9. https://link.springer.com/book/10.1007/978-3-030-83640-5.

Bobbio, A., Portinale, L., Minichino, M., Ciancamerla, E., 2001. Improving the analysis of dependable systems by mapping fault trees into bayesian networks. Reliab. Eng. Syst. Saf. 71, 249–260. https://doi.org/10.1016/S0951-8320(00)00077-6.

British Broadcasting Corporation, 2016. BBC website [WWW Document]. URL. http://www.bbc.com/news/world-middle-east-36563635in, 2016 (accessed 8.31.16).

Budescu, D.V., Chen, E., 2015. Identifying expertise to extract the wisdom of crowds. Manage Sci 61, 267–280. https://doi.org/10.1287/mnsc.2014.1909.

Cameron, I.T., Raman, Raghu, 2005. PROCESS SYSTEMS RISK MANAGEMENT, News. Elsevier, Ge. ISBN: 9780123995391.

Cockshott, J.E., 2005. Probability bow-ties a transparent risk management tool. Process Saf. Environ. Protect. 83, 307–316. https://doi.org/10.1205/psep.04380.

Dempster, A.P., 2008. The Dempster-Shafer calculus for statisticians. Int. J. Approx. Reason. 48, 365–377. https://doi.org/10.1016/j.ijar.2007.03.004.

Dempster, A.P., 1967. Upper and lower conditional probabilities induced by a multivalued mapping. Annuals of Mathematical Statistics 38, 325–339. https://doi.org/10.1007/978-3-540-44792-4_3.

Dubois, D., Prade, H., 1986. On the Unicity of Dempster Rule of Combination. *International.* Journal of Intelligent Systems 1 (2), 133–142. https://doi.org/10.1002/int.4550010204.

Estrada-Lugo, H.D., Santhosh, T.V., de Angelis, M., Patelli, E., 2020. Resilience assessment of safety-critical systems with credal networks. In: 30th European Safety and Reliability Conference, ESREL 2020 and 15th Probabilistic Safety Assessment and Management Conference, pp. 1199–1206. https://doi.org/10.3850/978-981-14-8593-0. PSAM 2020.

Faes, M.G.R., Daub, M., Marelli, S., Patelli, E., Beer, M., 2021. Engineering analysis with probability boxes: a review on computational methods. Struct. Saf. 93. https://doi.org/10.1016/j.strusafe.2021.102092.

Ferson, S., Ginzburg, L.R., 1996. Different methods are needed to propagate ignorance and variability. Reliab. Eng. Syst. Saf. 54, 133–144. https://doi.org/10.1016/S0951-8320(96)00071-3.

Ferson, S., Kreinovich, V., Ginzburg, L., Myers, D.S., Sentz, K., 2003. Constructing Probability Boxes and Dempster-Shafer Structures, vol. 143. Sandia National Laboratories. https://doi.org/10.2172/809606.

Gray, A., Ferson, S., Kreinovich, V., Patelli, E., 2022. Distribution-free risk analysis. Int. J. Approx. Reason. 146, 133–156. https://doi.org/10.1016/J.IJAR.2022.04.001.

Heydari, Z., Rahmani, V., Heydari, A.A., Motavassel, M., 2022. Risk assessment and risk management of kermanshah province gas Company using HAZOP method. Iran J. Oil Gas Sci. Technol 11, 28–37. https://doi.org/10.22050/IJOGST.2022.292733.1604.

Hosseinnia Davatgar, B., Paltrinieri, N., Bubbico, R., 2021. Safety barrier management: risk-based approach for the oil and gas sector. J. Mar. Sci. Eng. 9. https://doi.org/10.3390/jmse9070722.

GeNIe, 2019 2.4.4601 Academic Installer. Decision Systems Laboratory, University of Pittsburg. Available online from URL https://www.bayesfusion.com/.

Hugo, V., Rocha, N., Cozman, F.G., 2022. A Credal Least Undefined Stable Semantics for Probabilistic Logic Programs and Probabilistic Argumentation.19,309-319.doi: 10.24963/kr.2022/31.

International Electrotechnical Commission, 2006. IEC 60812: Analysis Techniques for System Reliability-Procedure for Failure Mode and Effects Analysis (FMEA), second ed. IEC Standards Online. https://webstore.iec.ch/en/publication/3571.

Jensen, F., 2001. Bayesian networks and decision graphs, First. Bayesian Networks and Decision Graphs. Springer, New York. https://doi.org/10.1007/978-1-4757-3502-4.

Jones, B., Jenkinson, I., Yang, Z., Wang, J., 2010. The use of Bayesian network modelling for maintenance planning in a manufacturing industry. Reliab. Eng. Syst. Saf. 95, 267–277. https://doi.org/10.1016/j.ress.2009.10.007.

Karimi, A., zarei, E., hokmabadi, R., 2022. Analyzing reliability of CGS station by continuous time Markov chains (CTMC). International Journal of Reliability, Risk and Safety: Theory and Application 4, 91–96. https://doi.org/10.30699/ijrrs.4.2.10.

Klawonn, F., Schwecke, E., 1992. On the Axiomatic Justification of Dempster's Rule of Combination.

Li, M., Wang, H., Wang, D., Shao, Z., He, S., 2020a. Risk assessment of gas explosion in coal mines based on fuzzy AHP and bayesian network. Process Saf. Environ. Protect. 135, 207–218. https://doi.org/10.1016/j.psep.2020.01.003.

Li, M., Wang, H., Wang, D., Shao, Z., He, S., 2020b. Risk assessment of gas explosion in coal mines based on fuzzy AHP and bayesian network. Process Saf. Environ. Protect. 135, 207–218. https://doi.org/10.1016/J.PSEP.2020.01.003.

Mauá, D.D., Cozman, F.G., 2020. Thirty years of credal networks: specification, algorithms and complexity. Int. J. Approx. Reason. 126, 133–157. https://doi.org/10.1016/j.ijar.2020.08.009.

Milazzo, M.F., Ancione, G., Consolo, G., 2021. Human factors modelling approach: application to a safety device supporting crane operations in major hazard industries. Sustainability 13, 1–20. https://doi.org/10.3390/su13042304.

Misuri, A., Khakzad, N., Reniers, G., Cozzani, V., 2018. Tackling uncertainty in security assessment of critical infrastructures: Dempster-Shafer Theory vs. Credal Sets Theory. Saf. Sci. 107, 62–76. https://doi.org/10.1016/j.ssci.2018.04.007.

Morais, C., Estrada-Lugo, H.D., Tolo, S., Jacques, T., Moura, R., Beer, M., Patelli, E., 2022. Robust data-driven human reliability analysis using credal networks. Reliab. Eng. Syst. Saf. 218, 107990. https://doi.org/10.1016/J.RESS.2021.107990.

Morais, C., Ferson, S., Moura, R., Tolo, S., Beer, M., Patelli, E., 2021. Handling the uncertainty with confidence in human reliability analysis 3312–3318. https://doi.org/10.3850/978-981-18-2016-8_575-cd.

Morais, C., Tolo, S., Moura, R., Beer, M., Patelli, E., 2019. Quantitative model evaluating the effect of novel decision support tool on the probability of ship-ship accident. In: Proceedings of the 30th European Safety and Reliability Conference. https://doi.org/10.3850/978-981-11-2724-3.

Mostafavi, S.A., Shirazi, M., 2020. Thermal modeling of indirect water heater in city gate station of natural gas to evaluate efficiency and fuel consumption. Energy 212, 118390. https://doi.org/10.1016/j.energy.2020.118390.

Nguyen, H.T., Safder, U., Kim, J.I., Heo, S.K., Yoo, C.K., 2022. An adaptive safety-risk mitigation plan at process-level for sustainable production in chemical industries: an integrated fuzzy-HAZOP-best-worst approach. J. Clean. Prod. 339, 130780. https://doi.org/10.1016/J.JCLEPRO.2022.130780.

Nourian, R., Mousavi, S.M., Raissi, S., 2019. A fuzzy expert system for mitigation of risks and effective control of gas pressure reduction stations with a real application. J. Loss Prev. Process. Ind. 59, 77–90. https://doi.org/10.1016/j.jlp.2019.03.003.

Pasman, H., Sun, H., Yang, M., Khan, F., 2022. Opportunities and threats to process safety in digitalized process systems—An overview 6 1–23. https://doi.org/10.1016/BS.MCPS.2022.05.007.

Patelli, E., 2015. COSSAN: a multidisciplinary software suite for uncertainty quantification and risk management. In: Handbook of Uncertainty Quantification. Springer International Publishing, pp. 1–69. https://doi.org/10.1007/978-3-319-11259-6_59-1.

Patelli, E., George-Williams, H., Sadeghi, J., Rocchetta, R., Broggi, M., de Angelis, M., 2018. OpenCossan 2.0: an efficient computational toolbox for risk, reliability and resilience analysis. In: Beck, André T., de Souza, Gilberto F.M., Marcelo, A. (Eds.), Proceedings of the Joint ICVRAM ISUMA UNCERTAINTIES Conference. Trindade. http://icvramisuma2018.org/cd/web/PDF/ICVRAMISUMA2018-0022.PDF.

Patelli, E., Pradlwarter, H.J., 2010. Global Sensitivity of Structural Variability by Random Sampling. Computer Physics Communications 181 (12), 2072–2081. https://doi.org/10.1016/j.cpc.2010.08.007.

Polavarapu, H.K., 2021. Integration of human factors in hazard identification and risk assessment. Process Safety Management and Human Factors 61–71. https://doi.org/10.1016/B978-0-12-818109-6.00006-X.

Qiao, W., Liu, Yu, Ma, X., Liu, Yang, 2020. Human factors analysis for maritime accidents based on a dynamic fuzzy bayesian network. Risk Anal. 40, 957–980. https://doi.org/10.1111/risa.13444.

Rafiee, B., Shishehbori, D., hoseini basab, H., 2019. Analyzing system safety and risks under uncertainty using failure mode and effect analysis approach and D-S evidence theory: application to city gate station. In: 16th Iran International Industrial Engineering Conference,Tehran. Undefined, Tehran.

Rafiee, B., Shishehbori, D., Hosseini nasab, H., 2020. Tackling uncertainty in safety risk analysis in process systems : the case of gas pressure reduction stations. Journal of Industrial and Systems Engineering 13, 1–15. http://www.jise.ir/article_111692.html.

Ramzali, N., Lavasani, M.R.M., Ghodousi, J., 2015. Safety barriers analysis of offshore drilling system by employing Fuzzy event tree analysis. Saf. Sci. 78, 49–59. https://doi.org/10.1016/j.ssci.2015.04.004.

Razavi, S., Jakeman, A., Saltelli, A., Prieur, C., Iooss, B., Borgonovo, E., Plischke, E., Lo Piano, S., Iwanaga, T., Becker, W., Tarantola, S., Guillaume, J.H.A., Jakeman, J., Gupta, H., Melillo, N., Rabitti, G., Chabridon, V., Duan, Q., Sun, X., Smith, S., Sheikholeslami, R., Hosseini, N., Asadzadeh, M., Puy, A., Kucherenko, S., Maier, H. R., 2021. The Future of Sensitivity Analysis: an essential discipline for systems modeling and policy support. Environ. Model. Software 137, 104954. https://doi.org/10.1016/J.ENVSOFT.2020.104954.

Rocchetta, R., Broggi, M., Patelli, E., 2018. Do we have enough data? Robust reliability via uncertainty quantification. Appl. Math. Model. 54, 710–721. https://doi.org/10.1016/J.APM.2017.10.020.

Ryu, B.R., Duong, P.A., Kim, J.-B., Choi, S.-Y., Shin, J.W., Jung, J., Kang, H., 2023. The effect of ventilation on the hazards of hydrogen release in enclosed areas of hydrogen-fueled ship. J. Mar. Sci. Eng. 11, 1639. https://doi.org/10.3390/jmse11091639.

Saltelli, A., Ratto, M., Andres, T., Campolongo, F., Cariboni, J., Gatelli, D., Saisana, M., Tarantola, S., 2008. Global Sensitivity Analysis: the Primer. John Wiley. https://doi.org/10.1002/9780470725184.

Schulman, P.R., 2023. Problems and paradoxes of reliability and resilience in organizational networks. Saf. Sci. 167, 106279. https://doi.org/10.1016/J.SSCI.2023.106279.

Sentz, K., Ferson, S., 2002. Combination of evidence in dempster- shafer theory. Tech. Rep. SAND, 2002-0835. Sandia National Laboratories. doi: 10.2172/800792. https://doi.org/10.2172/800792.

Shafer, G., 1976. A Mathematical Theory of Evidence. Princeton University Press. https://doi.org/10.1515/9780691214696.

Shenoy, P.P., 2023. Making inferences in incomplete Bayesian networks: a Dempster-Shafer belief function approach. Int. J. Approx. Reason. 160. https://doi.org/10.1016/j.ijar.2023.108967.

Tolo, S., Patelli, E., Beer, M., 2018. An open toolbox for the reduction, inference computation and sensitivity analysis of Credal Networks. Adv. Eng. Software 115, 126–148. https://doi.org/10.1016/j.advengsoft.2017.09.003.

Voorbraak, F., 1991. On the justification of Dempster's rule of combination. Artif. Intell. 48, 171–197. https://doi.org/10.1016/0004-3702(91)90060-W.

Yager, R.R., 1986. Arithmetic and other operations on Dempster-Shafer structures. Int. J. Man Mach. Stud. 25, 357–366. https://doi.org/10.1016/S0020-7373(86)80066-9.

Yan, F., Xu, K., 2019. Methodology and case study of quantitative preliminary hazard analysis based on cloud model. J. Loss Prev. Process. Ind. 60, 116–124. https://doi.org/10.1016/j.jlp.2019.04.013.

Yazdi, M., Khan, F., Abbassi, R., 2021. Microbiologically influenced corrosion (MIC) management using Bayesian inference. Ocean. Eng. 226, 108852. https://doi.org/10.1016/J.OCEANENG.2021.108852.

Zhao, K., Li, L., Chen, Z., Sun, R., Yuan, G., Li, J., 2022. A survey: optimization and applications of evidence fusion algorithm based on Dempster–Shafer theory. Appl. Soft Comput. 124, 109075. https://doi.org/10.1016/J.ASOC.2022.109075.